https://doi.org/10.5194/egusphere-2025-6208
Preprint. Discussion started: 4 January 2026

Thawing Siberian permafrost stabilizes organic carbon from recent plant litter inputs

Christian Knoblauch[1,2], Carolina Voigt[1,3], Christian Beer[1,2]

[1]University of Hamburg, Department of Earth System Sciences, Allende Platz 2, 20146 Hamburg, Germany

[2] University of Hamburg, Center for Earth System Research and Sustainability, 20146 Hamburg, Germany

[3]Alfred Wegener Institute Helmholtz Center for Polar and Marine Research, Permafrost Research Section, Telegrafenberg, 14473 Potsdam, Germany

Correspondence to: Christian Knoblauch (Christian.Knoblauch@uni-hamburg.de)

https://doi.org/10.5194/egusphere-2025-6208
Preprint. Discussion started: 4 January 2026

Abstract. Greenhouse gas release due to microbial decomposition of thawing permafrost organic matter receives ample attention but the other side of the permafrost soil carbon budget, the stabilization of organic matter due to rising plant litter input in a greening Arctic has hardly been addressed. Here we explore whether thawing permafrost may act as a long-term sink of fresh plant litter carbon. To identify the magnitude and drivers of litter carbon stabilization in thawing permafrost, we incubated permafrost samples under oxic and anoxic conditions with ^{13}C-labelled plant litter for nine years, used the microbial CO_2 and CH_4 production to calibrate a carbon decomposition model, and finally fractionated the remaining organic matter into a dissolved, a mineral-associated and a particulate fraction. At the end of the experiment, on average 38.9 ± 21.1 (mean ± SD, oxic) and 59.1 ± 12.2 % (anoxic) of the added litter-C was still present in the thawed permafrost. The mean residence times of the stable litter carbon pool of 17.6 (22.3) yr (median (IQR), oxic) and 52.4 (54.2) yr (anoxic) indicate a substantial stabilization of fresh litter carbon in thawing permafrost. Most of the remaining litter carbon (82.5 (35.3) % oxic and 83.8 (21.4) % anoxic) was part of the mineral-associated fraction, but in contrast to current understanding, litter decomposability is positively correlated with the size of the mineral bound litter pool. Although the fraction of mineral-bound permafrost carbon (64.4 (20.0) % oxic and 68.0 (17.0) % anoxic) was significantly smaller than of litter carbon, the mean residence times of the stable permafrost carbon pools were more than 10-fold higher. We identified interactions between new litter carbon and pre-existing mineral-bound permafrost carbon as an important driver of litter carbon stabilization. Such interactions may reduce net carbon emissions from thawing permafrost and add complexity to the permafrost carbon climate feedback.

1 Introduction

About 15–18 % of the land area of the northern hemisphere is underlain by permafrost, i.e. perennially frozen ground (Zhang et al., 2000; Obu et al., 2019). Soils in these circum-Arctic terrestrial landscapes store about 1300 Pg organic carbon, 800 Pg of which is preserved in the permafrost (Hugelius et al., 2014). The storage of such large amounts of organic matter (OM) is due to an imbalance between plant net primary productivity and microbial plant litter mineralization. The unique environmental conditions in the permafrost region facilitate the accumulation of OM, as low temperatures slow down OM decomposition. Furthermore, water-saturated, anoxic soils are widespread in the permafrost region since permafrost impedes water drainage. In these cold, waterlogged soils, microbial carbon decomposition is particularly low and OM accumulation is high (Heikkinen et al., 2002; Eckhardt et al., 2019).

The carbon dynamics in permafrost-affected soils differ fundamentally between the active layer, i.e. the surface soil layer that thaws every year, and the permafrost underneath. If vegetated, the active layer receives regular inputs of fresh OM from root exudates and decaying plant material, which are decomposed by microorganisms. Soil organic matter (SOM) is transported by cryoturbation and advection (Beer et al., 2022) into deeper soil layers where decomposition slows down (Kaiser et al., 2007) and SOM is ultimately stabilized through incorporation into permafrost (Ping et al., 2015). Although microbial activity may proceed at a low level even at sub-zero temperatures (Mikan et al., 2002; Natali et al., 2019), freezing conditions in the

https://doi.org/10.5194/egusphere-2025-6208
Preprint. Discussion started: 4 January 2026

permafrost largely protects SOM from decomposition, causing the persistence of labile OM for thousands of years without contact to fresh plant litter.

The strong warming of the Arctic, which is up to four times higher than the global average (Rantanen et al., 2022), causes the active layer to gradually deepen, but also induces abrupt thaw processes, particularly in ice-rich permafrost deposits (Turetsky et al., 2020). Such abrupt thaw processes induce fundamental changes in the land surface through thermo-erosion and exposes deep permafrost material to the surface (Lewkowicz and Way, 2019). Thawing permafrost liberates OM, which is decomposed by microorganisms to the greenhouse gases carbon dioxide (CO_2) and methane (CH_4) (Schädel et al., 2016; Knoblauch et al., 2018). But importantly, Arctic warming also causes longer growing seasons (Euskirchen et al., 2006; Arndt et al., 2019) with higher plant productivity (Natali et al., 2012; Berner et al., 2020) and increased inputs of plant litter (Elmendorf et al., 2012) as source for SOM formation.

The permafrost region has been a net carbon sink in the past, documented by the huge accumulation of organic carbon. Whether it will remain a carbon sink or turn into a carbon source depends on how primary productivity and OM decomposition respond to climate change. Current studies based on field flux measurements and modelling approaches indicate that the permafrost region may still be a weak carbon sink, at least in the boreal forest, but the tundra regions seem close to the threshold or have already switched to a net carbon source (Belshe et al., 2013; Virkkala et al., 2021; Hugelius et al., 2024). However, uncertainties remain high, also due to an incomplete understanding of long-term processes.

Although the decomposition of permafrost OM and the subsequent release of carbon has received ample attention (Elberling et al., 2013; Schädel et al., 2014; Drake et al., 2015; Faucherre et al., 2018; Gentsch et al., 2018; Beer et al., 2022; Guo et al., 2024), little is known about the stabilization of fresh plant litter in thawing permafrost, despite its potential impact on the long-term carbon budget. Thawing removes the freeze-induced stabilization of permafrost OM, increases the volume of the active layer, and allows fresh plant litter to be incorporated into SOM. Microbial SOM decomposition not only produces CO_2 and CH_4 but also promotes the stabilization of litter decay products and microbial necromass through different mechanisms such as physical protection or sorption onto mineral surfaces (Schmidt et al., 2011; Cotrufo et al., 2013; Begill et al., 2023; Qin et al., 2024). These processes and the factors determining the long-term persistence of OM from recent plant litter in thawing permafrost are poorly understood.

Soil organic matter is a mixture of organic material of different age, molecular composition and chemical properties. To simulate future carbon release from soils, organic matter decomposition models need to differentiate among several pools with different decomposability. Such process-based models are calibrated using experimentally determined OM decomposition rates (Tuomi et al., 2009; Schädel et al., 2014; Knoblauch et al., 2018). However, these models do not allow characterizing the composition of SOM or identifying the mechanisms of SOM stabilization. Therefore, physical SOM fractionation methods followed by the chemical analysis of the derived fractions are applied (Schrumpf et al., 2013; Torn et al., 2013; Prater et al., 2020; Martens et al., 2023). It has been shown that the OM associated with the mineral phase (MAOM) is generally older and has a higher C/N ratio than the particulate OM fraction (POM), indicating a higher decomposability or lability of the POM fraction (Torn et al., 2013; Prater et al., 2020; Martens et al., 2023). However, only a few studies have measured the microbial

https://doi.org/10.5194/egusphere-2025-6208
Preprint. Discussion started: 4 January 2026

decomposability of the different OM fractions in permafrost soils (Jagadamma et al., 2014; Gentsch et al., 2015a) and no clear difference in OM lability between these fractions was detected. On the other hand, carbon from plant litter may rapidly be incorporated into the mineral fraction (Swanston et al., 2005; Vogel et al., 2014; Haddix et al., 2016) but the lability of this recently bound OM remains largely unknown.

Our study, based on a nine years lasting incubation experiment with ^{13}C-labelled plant litter, aims to improve our understanding on two contrasting processes and their interaction after permafrost thaw: (1) the long-term stabilization of OM from decaying fresh plant litter in thawing permafrost and (2) the mineralization of old permafrost OM. We hypothesize that (h1) fresh plant litter is stabilized on mineral surfaces thereby contributing to the SOM build-up in thawing permafrost soils and that (h2) the persistence of mineral bound plant litter is lower than the persistence of mineral bound permafrost OM.

2 Materials and Methods

2.1 Sampling sites

Permafrost samples were collected from the uppermost 4.3 m of permafrost deposits from two islands in the Lena River Delta, Russia as described in Knoblauch et al. (2013). The island Kurungnakh (72.327503° N, 126.277597° E) is comprised of Pleistocene Yedoma deposits, which are covered by silty, cryoturbated Holocene sediments. Samples were taken at from a core drilled from the surface into the permafrost and from a headwall of a retrogressive thaw slump (Knoblauch et al., 2013; Bischoff et al., 2013) In contrast, Samoylov Island (72.369444° N, 126.475° E) is comprised mainly of sandy, fluviatile sediments that were deposited during the late Holocene. There, a permafrost core was drilled from the permafrost surface into a depth of 4.5 m. The tundra vegetation at both sites is composed of a moss/lichen layer and a grass/sedge layer. The dominant vascular plants in the wet tundra on Samoylov and Kurungnakh are sedge species of the *Carex aquatilis* aggregate (Kutzbach et al., 2004; Lashchinskiy et al., 2020).

Permafrost samples from Kurungnakh are characterized by relatively high organic carbon concentrations (33.9–121 mg C g^{-1}), intermediate C/N ratios between 12 and 19 and increasing pH values ranging from extremely acidic at the permafrost surface to neutral in the deepest layers (Knoblauch et al., 2013), (Appendix, Table A1). The texture of Kurungnakh permafrost is dominated by the silt fraction with generally more than 50 % and a relatively constant clay fraction slightly above 20 %. The organic carbon concentrations in the Samoylov permafrost (6–47 mg C g^{-1}) are lower than on Kurungnakh while the C/N values are higher (15–25). The pH values are relatively stable and in the slightly acidic range (Knoblauch et al., 2013), (Appendix, Table A1). The sand content of the Samoylov permafrost samples is decreasing from 85 % at the permafrost surface to 37 % in the deepest layer while the clay content ranges from 3 to 13 %.

2.2 Incubation experiment

The incubation experiment has been described in detail previously (Knoblauch et al., 2018). Briefly, twelve permafrost samples from Kurungnakh and Samoylov (Appendix, Table A1) were incubated in triplicate at 4° C under oxic and anoxic conditions

https://doi.org/10.5194/egusphere-2025-6208
Preprint. Discussion started: 4 January 2026

in 120 ml injection vials that were closed with butyl rubber stoppers and were not opened during the experiment to keep moisture constant (Appendix, Fig. A1). Anoxic conditions were established by repeatedly evacuating and flushing the headspace of the bottles with molecular nitrogen at the beginning of the experiment. The headspace of the oxic incubations was repeatedly flushed with synthetic air (20 % O_2, 80 % N_2) when CO_2 concentrations exceeded 3 %. During the first four years, labile OM was decomposed and an active methanogenic community developed in the anoxic incubations (Knoblauch et al., 2013). Data from this pre-incubation experiment are not considered in this manuscript. After four years, the amount of permafrost organic carbon (permafrost-C) that was mineralized to CO_2 and CH_4 in each of the samples was replenished with organic carbon from ^{13}C-labelled *Carex aquatilis* (litter-C) (Appendix, Table A1) that was grown on Samoylov Island. Such prepared permafrost samples contained two isotopically distinct carbon sources, the permafrost-C (-26.5 to -29.1 ‰ VPDB) and the litter-C (+774 ‰ VPDB). The samples were then incubated for a further nine years. Based on the different δ^{13}C-signatures of permafrost-C and litter-C, a two-endmember model was applied to quantify the amount of CO_2 and CH_4 produced from the two carbon sources permafrost-C and litter-C (Amundson and Baisden, 2000). Organic matter decomposition rates were calculated from three successional measurements at the beginning (initial rates) and end (final rates) of the incubations, and were related to the concentration of the respective carbon source present at the respective time interval.

2.3 Gas quantification and carbon stable isotope analysis

The production of CO_2 and CH_4 was quantified by measuring the gas pressure (LEO1, Keller Druckmesstechnik, Switzerland), and gas concentrations in the headspace of the incubation flasks with a gas chromatograph (GC 7890, Agilent Technologies, USA) as described before (Knoblauch et al., 2018).

The δ^{13}C-values of CO_2 and CH_4 were determined with an isotope ratio mass spectrometer (Delta V, Thermo Fischer Scientific, Bremen, Germany) equipped with a GC Isolink (Thermo Fischer Scientific, Milano, Italy). CH_4 was measured against the external standards NIST 8561 (-73.27 ‰ VPDB) and USGS HCG-1 (-1.51 ‰ VPDB) while CO_2 was measured against LSVEC (-46.60 ‰ VPDB), CO-8 (-5.76 ‰ VPDB) and IAEA 303A (+93.3 ‰ VPDB). Stable carbon isotope analysis of particulate organic carbon and DOC were carried out with a Delta VPlus isotope ratio mass spectrometer and a ConFlo IV (ThermoFisher Scientific, Bremen, Germany) that was connected to a Flash EA (ThermoFisher Scientific, Bremen, Germany) for δ^{13}C-analysis of carbon in the bulk samples, the POM and the MAOM fraction, and with an Aurora 1030 (OI Analytical, Yellow Springs, USA) for δ^{13}C-DOC analyses. ^{13}C-analysis of DOC and solid samples were calibrated against the isotope standards IAEA-CH-7 (-10.45‰ VPDB), USGS40 (-26.39‰ VPDB) and USGS41 (+37.63‰ VPDB).

2.4 Soil analysis

Total carbon and nitrogen in the bulk samples and the POM and MAOM fractions were determined with an elemental analyser (VarioMAX Elementar Analysensysteme GmbH, Hanau, Germany). If the available sample amount was too small, carbon analysis was conducted with the Flash EA in parallel to δ^{13}C-analysis. Carbon and nitrogen concentrations were calibrated against external standards with carbon concentrations between 48.3 % and 2.2 % and nitrogen concentrations between 2.30 %

https://doi.org/10.5194/egusphere-2025-6208
Preprint. Discussion started: 4 January 2026

and 0.20 % (IVA Analysentechnik, Meerbusch, Germany). Soil texture was determined by sieving and sedimentation (Iso 11277, 2002). Therefore, air dried soil (< 2 mm) was suspended in a 0.1 M $Na_4P_2O_7$ solution and sieved through a 63 µm mesh sieve. The retained fraction was dried at 105° C and subsequently fractionated by sieving through 630 µm, 200 µm, 125 µm, and 63 µm mesh sieves. The fraction of < 63 µm was separated by sedimentation using a Sedimat 4-12 (UGT, Müncheberg, Germany). Organic matter was destroyed with a 30 % H_2O_2 solution prior to texture analysis.

2.5 Organic matter fractionation

At the end of the incubation, the dissolved organic matter (DOM) was extracted from each of the replicates by mixing air dried soil with 0.01 M $CaCl_2$ solution (1:2; w:v), overhead shaking for 15 minutes and centrifugation for 30 minutes at 3000 g. The supernatant was filtered through a GFF filter, acidified to pH 2, and stored at 4° C until analysis. Subsequently, the OM from each replicate of each permafrost sample was separated by density fractionation. Due to the low amount of sample (7 – 15 g) we separated only two fractions, the POM and the MAOM. Dry permafrost samples were mixed with a Na-polytungstate solution (TC Tungsten Compounds, Grub am Forst, Germany) with a density of 1.6 g cm^{-3} (Cerli et al., 2012) at a ratio of 1:5 (w:v). To break up aggregates we used a sonication with 200 J ml^{-1} (Sonoplus HD 200 / Sonotrode MS 70, Bandelin, Berlin, Germany) in an ice bath. Subsequently, the samples were centrifuged at 2000 g for 30 minutes and the floating material (POM) was carefully separated from the sedimented material (MAOM) with a vacuum pump. The POM fraction was washed with deionized water by pressure filtration until the electrical conductivity in the washing solution decreased below 50 µS. Subsequently the POM fraction was detached from the filter (0.22 µm PVDF membrane, Berrytec, Harthausen, Germany) by ultrasonication and subsequently dried at 60° C. The MAOM fraction was washed by centrifugation (6000 g) with deionized water until the electrical conductivity in the washing solution decreased below 50 µS. The sediment with the MAOM fraction was then dried at 60° C. The median carbon recovery, i.e. the sum of carbon in the DOM, POM and MAOM fraction divided by the total organic carbon in the unfractionated sample was 96.2 % (IQR 10.4). The share of carbon in the three different OM fractions (DOM, POM, MAOM) to the total permafrost-C and litter-C was calculated by dividing the amount of carbon in the respective fraction through the total amount of carbon recovered.

2.6 Organic matter dynamic decomposition model

The cumulative CO_2 and CH_4 production from thawed permafrost-C and litter-C from each sample and replicate were used to calibrate an organic carbon decomposition model as described before (Knoblauch et al., 2013). The model follows the principles of the Introductory Carbon Balance Model (Andrén and Kätterer, 1997). A first-order kinetics equation represents the change of organic carbon content in time. This equation is applied to two carbon pools with a high and a low rate constant, respectively. The initial fraction of the labile pool is treated as a parameter and the initial fraction of the stable organic carbon pool is then calculated as the difference to the total organic carbon content. Using a nonlinear least-squares approach with a trust-region-reflective algorithm in MATLAB R2023b (MathWorks Inc., USA), the following four model parameters were optimized: two decomposition rate constants (labile and stable pool), initial labile carbon pool fraction, and the stabilization

https://doi.org/10.5194/egusphere-2025-6208
Preprint. Discussion started: 4 January 2026

coefficient. Mean residence time of each pool (MRT) is defined as the reciprocal of the decomposition rate constant. Replicates for which the model did not find reasonable fitting parameters (oxic n= 3, anoxic n= 10) were excluded.

2.7 Statistics

Prior to all analyses, data were inspected visually for their distribution via histograms, QQ-plots and by a Shapiro-Wilk test. Mean values were compared using a two-sided independent t-test. In the case of non-normal distribution, the medians were tested using a Mann-Whitney rank sum test or a Kruskal-Wallis ANOVA. Significance was tested on a level of $p<0.05$, using the Bonferroni correction in case of multiple tests. If mean values are presented, they are followed by the standard deviation (±SD), in case of medians they are followed by the interquartile range (IQR). Since most of the data did not show a normal distribution, we used for the correlation analysis a Spearman rank order correlation. Due to the correlation between the sand, silt, and clay fractions, the clay fraction was included as the single variable to represent soil texture. These statistical analyses were conducted with IBM SPSS Statistics 29.0 (IBM Corporation, Armonk, USA).

All further statistical analyses were performed in R version 4.3.2. To identify the most important controls on organic matter stabilization we applied a random forest (RF) machine learning approach. Input variables for the RF analyses were selected based on stepwise linear regression using R-package MuMIn (Bartón, 2023). Values were standardized using z-score scaling [(x - mean)/standard deviation]. The best linear model was selected based on the lowest Akaike Information Criterion, a Delta value < 2 and ≥ 6 degrees of freedom to obtain a sufficient number of variables for the subsequent RF analysis. Stepwise linear regression analysis was conducted for eight separate models using the following dependent variables: Fraction of litter-C decomposed, fraction of permafrost-C decomposed, MRT stable litter-C pool, MRT stable permafrost-C pool. The most important predictors for these dependent variables were identified separately for oxic and anoxic samples. Results of the stepwise-linear regression are listed in Appendix, Table A2. For the subsequent RF analysis, models for oxic and anoxic samples were merged to include the same set of predictor variables. The clay fraction was included as the single variable to represent soil texture. RF models were constructed for the same eight models created in the stepwise linear regression using the R-package randomForest (Breiman, 2001). We used 500 trees (ntree = 500) to create the random forests, and the function 'tuneRF' was applied to determine the number of variables tried at each split individually for each of the eight models. Highly-correlated variables (Spearman's correlation coefficient > 0.9) were excluded from the RF models. Variable importance was assessed using the average increase in node purity of the regression trees based on splitting on the various environmental variables (Louppe et al., 2013). The predictive power in the RF analysis was high (54–92 % explained variance) except for the MRT of the stable pool of permafrost-C under anoxic conditions for which the RF model barely converged at 6.5 % explained variance. Due to the relatively small number of observations in our dataset, we used partial dependence plots (R-package pdp) to assess the validity of the assumed responses (Appendix Fig. A2).

https://doi.org/10.5194/egusphere-2025-6208
Preprint. Discussion started: 4 January 2026

3 Results

3.1 Mineralization of litter carbon versus permafrost carbon

At the beginning of the incubation experiment, litter-derived CO_2 and CH_4 dominated gaseous carbon production. Initial litter-C mineralization rates were 35 (IQR 41) and 165 (168) times higher than initial permafrost-C mineralization rates under oxic and anoxic conditions, respectively, with about 60 % of total litter-C mineralization taking place in the first year (Appendix, Fig. A1a, Table A3). After one year, mineralization rates of litter-C decreased significantly more rapidly (t-test, $p<0.001$) than those of permafrost-C reaching median rates after nine years that represented only 9.3 (12.6) % and 1.5 (3.0) % of the initial rates under oxic and anoxic conditions, respectively. However, the median OM mineralization rates of litter-C at the end of the experiment were still about ten times higher than those of the remaining permafrost-C under both oxic and anoxic conditions (Appendix, Table A3).

The fraction of total litter-C that was decomposed during the incubation period ranged from 23 % to 97 % (mean 61±21 %) under oxic conditions and was significantly higher (t-test, $p<0.001$) than under anoxic conditions (mean 41±12 %, Fig. 1a). The fraction of permafrost-C that was decomposed was significantly lower than that of litter-C, ranging between 1.3 % and 16.3 % (median 4.8 %) under oxic conditions and between 0.5 % and 4.4 % (median 1.0 %) under anoxic conditions (Fig. 1b).

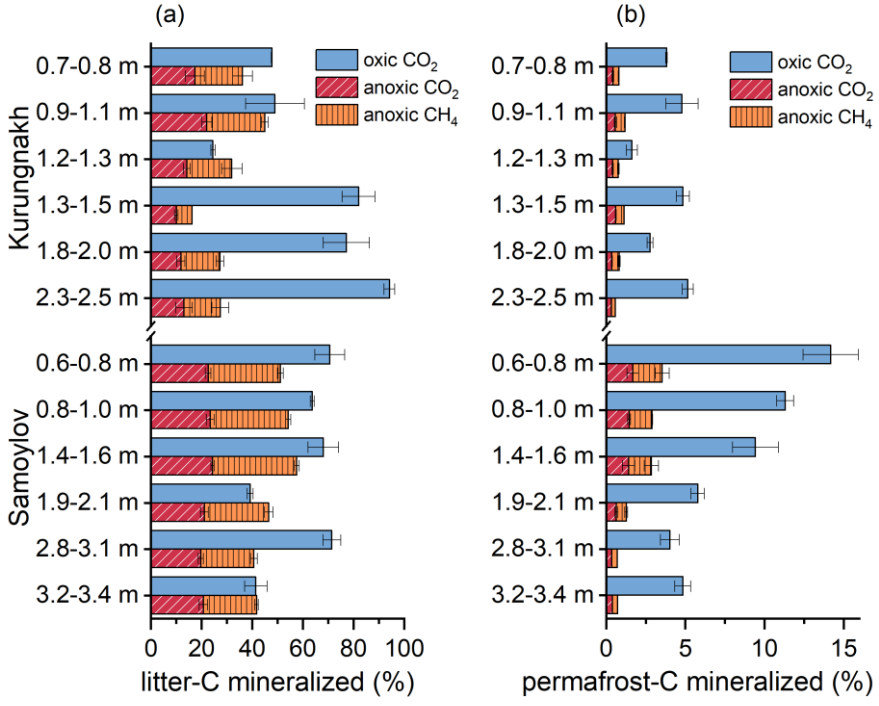

Figure 1: Total amount of organic carbon decomposed into CO_2 and CH_4 from litter-C (a) and permafrost-C (b) over nine years in samples incubated under oxic and anoxic conditions. Values are relative to the total amount of litter-C and permafrost-C at the beginning of the experiment. Error bars represent one standard deviation of the mean (n=3).

https://doi.org/10.5194/egusphere-2025-6208
Preprint. Discussion started: 4 January 2026

The median size of the labile litter-C pool, as determined by the two-pool carbon decomposition model (55 % oxic, 42 % anoxic; Fig. 2a) was close to the amount of litter-C that was decomposed during the incubation experiment. The size of the labile permafrost-C pools (7.3 % oxic, 1.2 % anoxic) was significantly smaller than the labile litter-C pools but also close to the amount of permafrost-C decomposed during the experiment. Therefore, while litter-C was dominated by the labile C-pool, at least under oxic conditions, permafrost-C comprised mainly stable carbon (Fig. 2c).

The MRT of the labile carbon pools of litter-C and permafrost-C were similar, with median values below 0.5 years, except for the labile permafrost-C pool under anoxic conditions with a significantly higher median MRT (Kruskal-Wallis ANOVA, $p = 0.004$; Fig. 2b). However, the median MRT of the stable permafrost-C pool was more than ten times higher than that of the stable litter-C pool, both under oxic conditions (195 yr vs. 17.6 yr) and anoxic conditions (1572 yr vs 52.4 yr) (Fig. 2d).

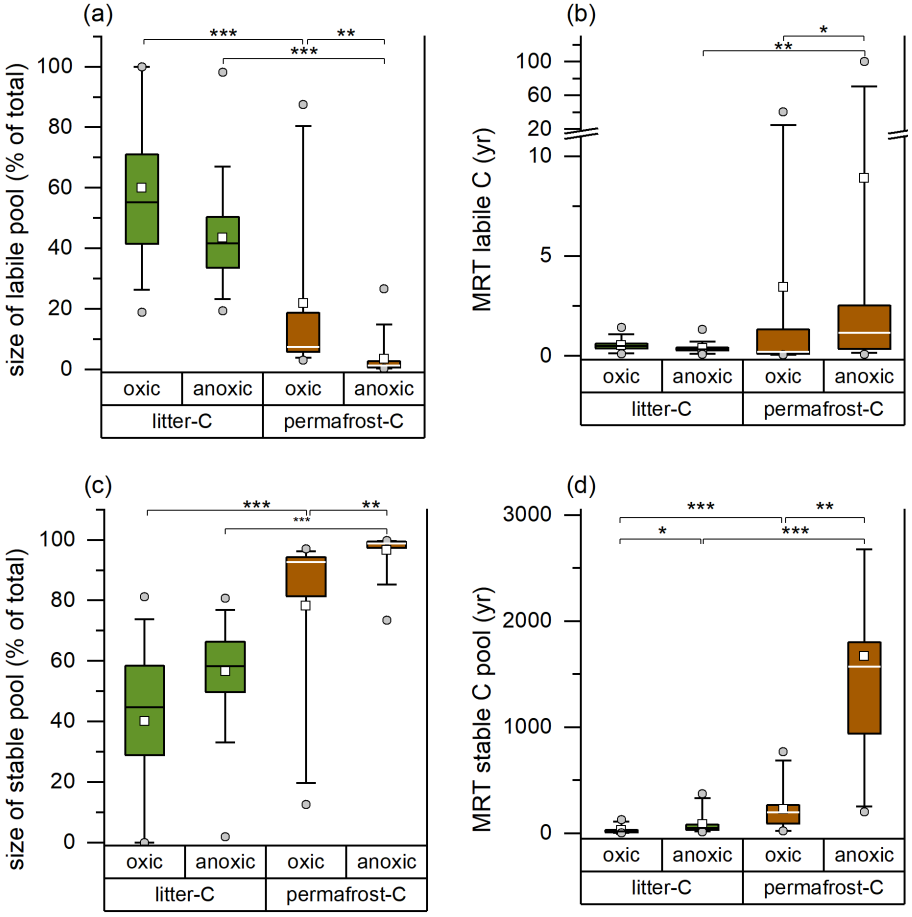

Figure 2: Size of the labile (a) and stable (c) litter-C and permafrost-C pools and mean residence times (MRT) of the respective carbon pools (b, d) determined by a two-pool carbon decomposition model. Significant differences are indicated by * = $p < 0.05$, ** = $p < 0.01$ and *** = $p < 0.001$ (Kruskal-Wallis ANOVA). The Box shows the 25/75 percentiles, the whiskers the 5/95 percentiles, the horizontal line the median and the closed square the mean. Outliers are presented as open circles.

https://doi.org/10.5194/egusphere-2025-6208
Preprint. Discussion started: 4 January 2026

The median ratio of initial oxic to anoxic litter mineralization rates was 3.6 (7.2) but this increased substantially to 8.0 (4.7) towards the end of the experiment. A similar increase was observed for the oxic/anoxic ratios for permafrost-C decomposition, rising from an initial ratio of 3.3 (1.3) to a final ratio of 6.9 (4.9).

3.2 Fractionation of permafrost carbon and litter carbon

Most organic carbon from both carbon sources remaining at the end of the incubations was found in the mineral-associated (MA) fraction (Fig. 3a, b). The median C/N ratio of 15.7 in the total MAOM fraction (sum of MA-permafrost-C and MA-litter-C) was significantly lower than the ratio of 29.5 in the total POM fraction.

The median values for mineral-associated permafrost-C under oxic and anoxic conditions were 64.4 (20.0) % and 68.0 (17.0) %, respectively (Fig. 3b). Surprisingly, we found a significantly higher proportion of litter-C remaining after nine incubation years in the mineral-associated fraction: 82.5 (35.3) % under oxic conditions and 83.8 (21.4) % under anoxic conditions (Fig. 3a). The median contribution of DOC to total permafrost-C and litter-C was generally below 1 %, except for the dissolved litter-C under anoxic conditions, which contributed 4.6 % to the total litter-C (Appendix Fig. A3).

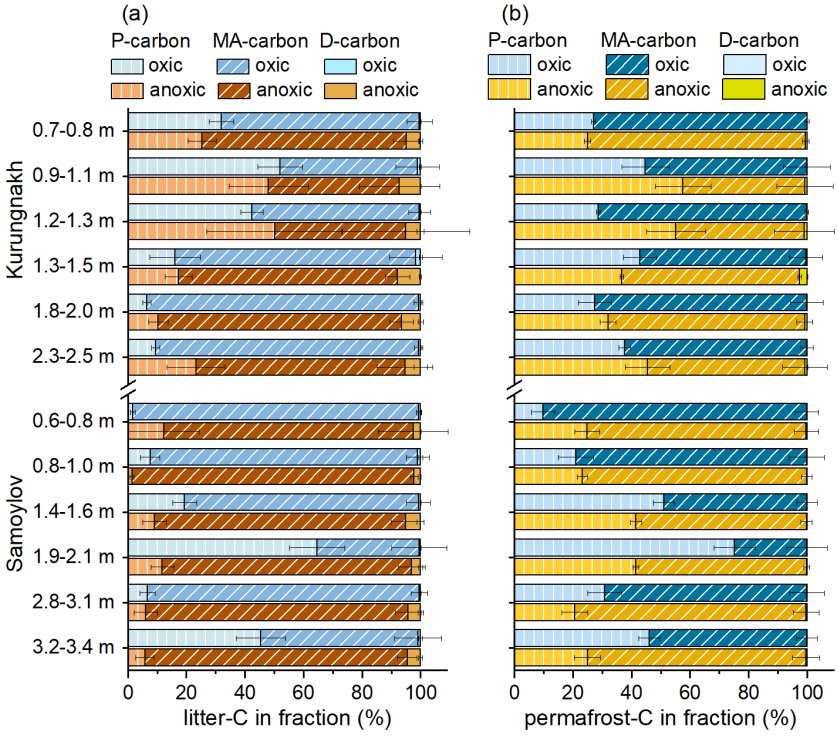

Figure 3: Contribution of litter-C (a) and permafrost-C (b) to the particulate (P-carbon), the mineral associated (MA-carbon) and the dissolved (D-carbon) carbon fractions in permafrost samples from Kurungnakh and Samoylov. Error bars representing one standard deviation of the mean (n = 3) are presented to the right of the respective bar.

https://doi.org/10.5194/egusphere-2025-6208
Preprint. Discussion started: 4 January 2026

3.3 Factors affecting organic carbon stabilization

The final permafrost-C decomposition rate, which was calculated based on the amount of carbon remaining at the end of the incubations, was the most important predictor of the parameters used to describe permafrost-C stabilization, i.e. the fraction of permafrost-C mineralized and the MRT of the stable pool of permafrost-C (Fig. 4). Texture, represented by the size of the clay fraction, was also an important predictor of not only permafrost-C and total nitrogen concentrations, but also of the fraction of permafrost-C decomposed and the MRT of the stable permafrost-C pool. Furthermore, the size of the clay fraction was negatively correlated with the final permafrost-C decomposition rates. However, the size of the MA-permafrost-C pool did not correlate with any of the parameters related to the decomposition of permafrost-C such as permafrost-C decomposition rates, the fraction of permafrost-C decomposed or the MRT of the stable permafrost-C pool (Fig. 4a). In the RF model (Fig. 4 d, e), the size of the mineral-associated permafrost-C was also one of the least important parameters explaining permafrost-C stabilization.

The final litter-C decomposition rates were the most important predictor of both the fraction of litter-C decomposed and the MRT of the stable litter-C pool (Fig. 4a, b, c). But surprisingly, and contrary to permafrost-C decomposition, the fraction of litter decomposed correlated positively with the proportion of MA-litter-C, which was also the parameter in the RF-model explaining most of the variance of the data under oxic conditions. Additionally, the proportion of MA-litter-C correlated negatively with the MRT of the stable litter-C pool; that is to say, the more litter-C that was bound to the mineral fraction, the lower the MRT of the stable C-pool. Texture was only a minor predictor of litter stabilization, since the size of the clay fraction only correlated with the parameters of litter stabilization under anoxic conditions, and only under anoxic conditions did the size of the clay fraction explain a substantial fraction of the data variance in the RF-model (Fig. 4 b, c). Interestingly, the proportion of MA-litter-C showed a strong positive correlation with the proportion of MA-permafrost-C both under both oxic and anoxic conditions.

https://doi.org/10.5194/egusphere-2025-6208
Preprint. Discussion started: 4 January 2026

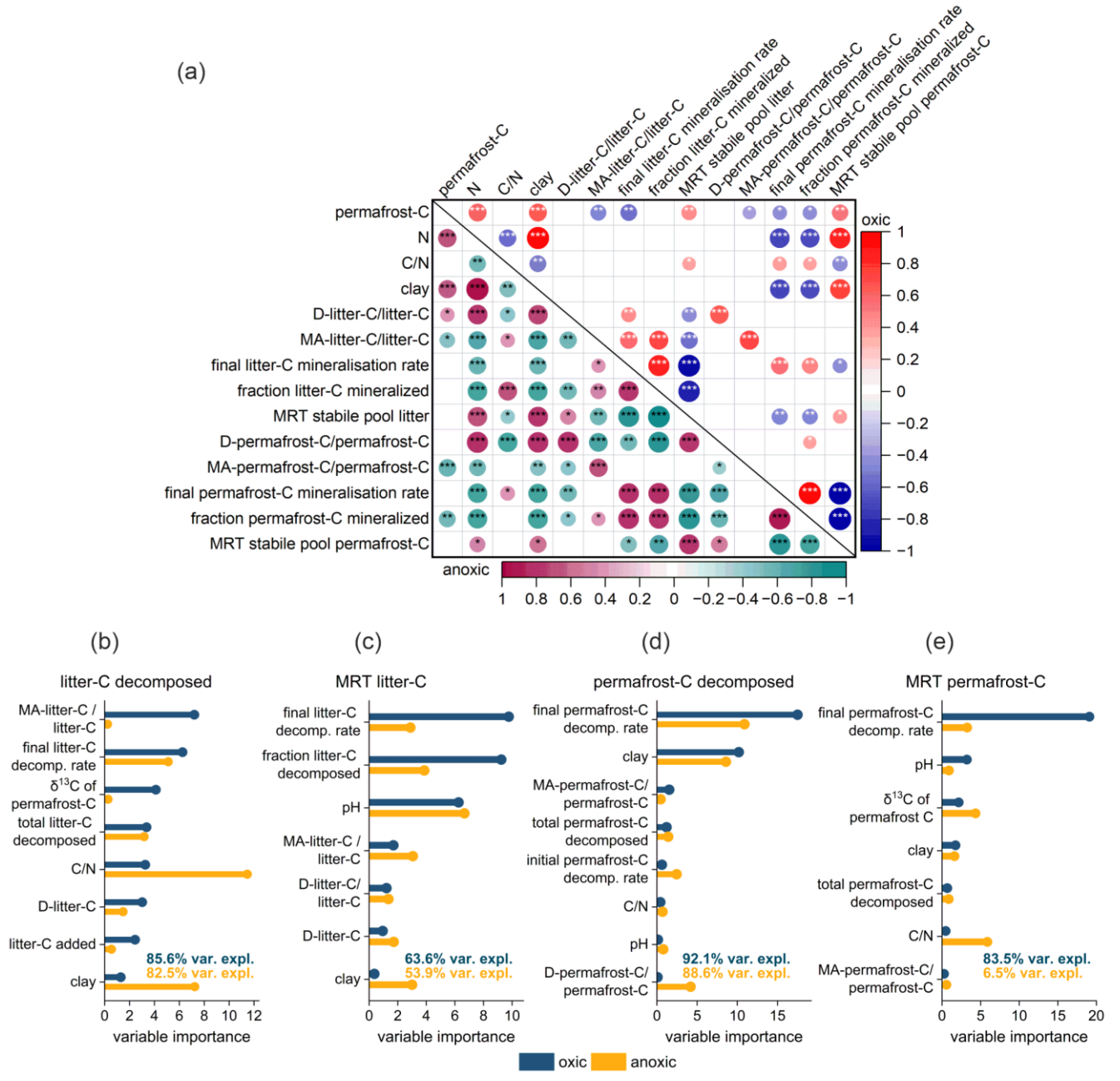

Figure 4: (a) Correlation table showing Spearman's correlation coefficients between soil properties and the fraction of permafrost-C and litter-C decomposed and the MRT of the stable pool of litter-C and permafrost-C. Results from samples incubated under oxic conditions are presented in the top right-hand corner, and results from anoxic incubations are presented in the bottom left-hand corner. The colours and size of the circles code the size of the correlation coefficient, the asterisk indicates the probability values with * = $p < 0.05$, ** = $p < 0.01$, *** = $p < 0.001$. (b) Relative importance of predictors on the fraction of litter-C decomposed, (c) the mean residence time (MRT) of stable litter-C pool, (d) the fraction of permafrost-C decomposed and (e) the MRT of the stable permafrost-C pool under oxic and anoxic conditions. The relative importance was determined with a random forest model for the individual treatments. For the direction of responses see Appendix Fig. A2a-d. Numbers in panels b-e give the percentage of variance in the data explained by the model.

https://doi.org/10.5194/egusphere-2025-6208
Preprint. Discussion started: 4 January 2026

4 Discussion

4.1 Organic matter decomposability

The high initial carbon mineralization rates of the added plant litter demonstrate the high share of labile OM in the *Carex aquatilis* litter that may readily be mineralized, as well as a microbial community adapted to the substrate and the low incubation temperature of 4° C. Litter-C loss during the nine-year incubation period is similar to the carbon loss from different sedges (44.7–61.0 %) incubated for two years under in situ conditions in Arctic soils (Cornelissen et al., 2007). However, the 90 % decrease of litter-C decomposition rates towards the end of the incubation indicates that 40–60 % of the added litter-C will resist a rapid decomposition.

In contrast, the carbon loss from permafrost-C of our Siberian permafrost samples (0.5–16 %) is at the lower end of the range (9–75 %) reported for a similar 12-year oxic incubation experiment with three permafrost soil samples from Greenland (Elberling et al., 2013). Prior to adding litter-C to our permafrost samples, they were pre-incubated for four years until the most labile permafrost-C had been mineralized (Appendix, Fig. A1) (Knoblauch et al., 2013). Including the carbon loss during this four-year pre-incubation period increases the permafrost-C loss over the 13-year incubation period to a median of 11 % (oxic) and 2.3 % (anoxic) in our study. Decade-long incubation experiments with permafrost soils are extremely rare but simulations of oxic carbon decomposition over ten incubation years based on data from over 120 samples from the circum-Arctic permafrost region indicate a wide range of carbon loss between 0.7 and 75 % with a median value of 7.5 % of the initial soil organic carbon content (Schädel et al., 2014). Therefore, our permafrost samples seem to represent the median permafrost OM decomposability rather than the reported extremes. Since the amount of carbon mineralized over the incubation period match the size of the labile carbon pools from both litter-C and permafrost-C we conclude that the carbon left at the end of the incubation mainly represents the stable carbon pools of both carbon sources.

The about tenfold difference between final litter-C and permafrost-C mineralization rates and between the MRT of stable carbon pools indicate different properties of OM from permafrost and of the remaining plant litter. The MRT of the stable litter-C is in the order of decades, consistent with the carbon turnover time of tundra ecosystems (Carvalhais et al., 2014). In contrast, the MRTs of centuries to millennia of the stable permafrost-C pool, which represents more than 90 % of total permafrost-C, disagree with reports of high amounts of labile, rapidly decomposable OM in permafrost deposits, which were identified using the chemical composition of permafrost OM (Waldrop et al., 2010; Mueller et al., 2015), differences in carbon contents between frozen and unfrozen sediments (Vonk et al., 2012) or incubation experiments over relatively short time periods (Waldrop et al., 2010). Initial high OM decomposition rates in thawing permafrost may be due to the elevated amount of DOC in permafrost, which is rapidly decomposed upon thaw (Vonk et al., 2013; Drake et al., 2015). However, data from oxic long-term (≥1 year) incubation studies from more than 20 permafrost affected circum-Arctic study sites show a significantly higher OM decomposability in the uppermost 1 m surface soil, comprising the active layer, than from the permafrost located below 1 m (Schädel et al., 2014). Similar results were obtained by incubating over 100 samples from permafrost affected soil profiles (Faucherre et al., 2018). Therefore, current long-term OM decomposition measurements are

https://doi.org/10.5194/egusphere-2025-6208
Preprint. Discussion started: 4 January 2026

consistent with our findings of a relatively low long-term decomposability of permafrost OM. One explanation for the lower decomposability of permafrost OM than active layer OM is likely the incorporation of subsoil OM into the permafrost. Even when containing cryoturbated material, subsoil OM is generally more decomposed than surface active layer material that receives an annual input of fresh plant litter (Schädel et al., 2014).

In our experiments, the initial ratio of oxic to anoxic carbon-based litter mineralization rates was similar to the ratio of 3.4 reported for a wide range of permafrost soil incubations (Schädel et al., 2016). However, the substantial increase of this ratio towards the end of the experiment proves a stronger decrease of anoxic than oxic OM decomposition rates over time. The lower decomposability of OM under anoxic versus oxic conditions is well established (Bridgham et al., 1998; Schädel et al., 2016) and likely due to the lower energy yield of microbial OM decomposition in the absence of oxygen (Larowe and Van Cappellen, 2011). Further reasons for a lower microbial activity in the absence of oxygen are the inhibition of hydrolytic enzymes by accumulating end products (Freeman et al., 2001) and the absence of oxygenase activity (Sinsabaugh, 2010), which breaks down refractory organic compounds such as lignin. However, similar decomposition rates under oxic and anoxic conditions have repeatedly been observed in short-term incubations and during the initial phase of OM decomposition (Bastviken et al., 2001; Lin et al., 2021; Knoblauch et al., 2021) indicating that labile OM may support high anoxic decomposition rates. Such labile OM may originate from fresh plant litter or from the reduction of iron(III) (oxoyhydr)oxides and the subsequent release of co-precipitated OM (Patzner et al., 2020). A similar decomposability of labile litter OM under oxic and anoxic conditions is supported by similar MRT of the labile litter-C pool in our incubations in the presence and absence of oxygen (Fig. 2b). Nevertheless, over longer time scales, decomposition rates under anoxic conditions are lower than those under oxic conditions as observed in our incubation study, causing significantly higher MRT and the highest carbon accumulation in water saturated soils (Köchy et al., 2015). The recalcitrance of OM in soils, i.e. its long-term persistence due to its molecular composition, has been questioned, as even lignin and lipids may rapidly be decomposed in oxic, well drained soils (Marschner et al., 2008). However, recalcitrance appears to matter still under anoxic conditions, as supported by the MRT of millennia in our anoxic incubations of permafrost-C and the large amounts of old particulate OM in peatlands, not stabilized by interaction with minerals or occluded in soil aggregates (Yeloff et al., 2006).

4.2 Properties of persistent organic carbon

The significantly higher C/N ratio of the POM in comparison to the MAOM remaining at the end of the incubations indicate different properties of the OM in these two fractions. The C/N ratio has been used as an indicator of OM decomposition (Schädel et al., 2014; Kuhry and Vitt, 1996) as C/N ratios of SOM decrease during on-going decomposition (Bonanomi et al., 2013; Gentsch et al., 2015b), which would indicate that the MAOM fraction contains more decomposed OM. However, lower C/N ratios in the MAOM than the POM fraction may also be caused by different sources of OM of the two fractions (Haddix et al., 2016), with a preferential accumulation of microbial necromass, with generally low C/N ratios, in the MAOM fraction (Wang et al., 2020) and a relative accumulation of refractory structural plant components such as lignin with a high C/N ratio in the POM fraction (Cheng et al., 2023). As we lack data on the sources of the OM in the different fractions, e.g. through

https://doi.org/10.5194/egusphere-2025-6208
Preprint. Discussion started: 4 January 2026

lignin or microbial biomarkers (Angst et al., 2021), we cannot substantiate either explanations for the higher C/N ratio in the POM fraction.

The proportion of mineral-associated permafrost-C under oxic and anoxic conditions, ranging from 60 to 70 %, falls within the values previously reported for Siberian permafrost (Beer et al., 2022; Martens et al., 2023; Gentsch et al., 2015b) as well as for deeper permafrost (>~80 cm) in drained thermokarst lake basins in Alaska (Mueller et al., 2015). In contrast, the active layer may be dominated by the POM fraction (Prater et al., 2020; Mueller et al., 2015), probably due to repeated input of POM through decaying plant litter. The surprisingly high share of more than 80 % of litter-C remaining after nine incubation years in the mineral-associated fraction indicates an efficient incorporation of plant-litter decomposition products and microbial necromass into the mineral fraction (Swanston et al., 2005; Haddix et al., 2016). However, this is also likely due to a preferential decomposition of POM resulting in a relative accumulation of mineral-associated litter-C (Cheng et al., 2023; Haddix et al., 2020).

Although the DOC pool is substantially smaller than the particulate and the mineral-associated carbon pools in permafrost soils, as shown in this and previous studies (Xu et al., 2009), it plays a central role in the decomposition and stabilization of organic matter since it is highly mobile, fastest decomposable (Vonk et al., 2013; Drake et al., 2015) and both the source for greenhouse gases when decomposed by microbes but also for OM stabilized at mineral surfaces (Cotrufo et al., 2013). The significantly higher concentrations of DOC from litter than from permafrost-C provide further evidence of the relatively higher lability of the remaining litter-C compared to permafrost-C.

4.3 Control of organic carbon stabilization

We use the MRT of the stable carbon pools and the fraction of litter-C or permafrost-C decomposed as indicators of organic carbon stabilization. The fact that the final mineralization rates of litter-C and permafrost-C were the most important predictors of carbon stabilization, while the initial mineralization rates provided little additional information, highlights the importance of long-term incubations when studying OM stabilization. Among the soil properties, it was mainly the size of the clay fraction that affected permafrost-C stabilization. The central role of clay for organic matter stabilization is well established (Kögel-Knabner et al., 2008), primarily because it provides a large mineral surface area for binding organic matter to form MA-permafrost-C (Gentsch et al., 2015a). The MAOM is generally considered to be the least decomposable and therefore most stable fraction of organic matter in soils (Kögel-Knabner et al., 2008; Mueller et al., 2015; García-Palacios et al., 2024). This interpretation is mainly based on observations of lower C/N ratios, lower ^{14}C-content and lower abundance of functional groups associated with labile OM in the MAOM fraction (Mueller et al., 2015; Beer et al., 2022; Prater et al., 2020). Although we found a significantly lower C/N ratio in the MAOM than in the POM fraction, indicative for a higher grade of degradation (Schädel et al., 2014; Kuhry and Vitt, 1996) and a contribution of microbial necromass to the MAOM fraction (Wang et al., 2020), the size of the MA-permafrost-C pool did not contribute to the explanation of permafrost-C stabilization. Therefore, our long-term decomposition experiment provided no evidence that the MAOM pool in permafrost is the most resistant or that the size of the POM pool can be used as an indicator of the amount of labile, fast-decomposable OM in permafrost. The few

https://doi.org/10.5194/egusphere-2025-6208
Preprint. Discussion started: 4 January 2026

existing, direct measurements of the decomposability of MAOM in comparison to POM or bulk OM in permafrost soils showed that MAOM in the surface active layer is significantly less decomposable than POM or bulk OM but that this is not the case for MAOM in permafrost (Gentsch et al., 2015a; Gentsch et al., 2018). The reason for the lack of difference between permafrost MAOM and POM degradability may lie in the generally lower decomposability of permafrost OM in comparison to OM from the active layer (Schädel et al., 2014), as well as in the dominance of permafrost POM occluded in aggregates (Martens et al., 2023; Beer et al., 2022), which makes the latter POM fraction less accessible to microbial decomposition.

The factors affecting litter-C stabilization differed from those affecting permafrost-C stabilization, with the exception that the final litter decomposition rate was also one of the most important predictors for both the fraction of litter decomposed and the MRT of the stable litter-C pool. Contrary to previous findings showing that the mineral fraction contains the most stable carbon in soils (Kögel-Knabner et al., 2008; Mueller et al., 2015; García-Palacios et al., 2024; Heckman et al., 2022; Schrumpf et al., 2013; Qin et al., 2021) our study revealed a decrease in litter-C stabilization with an increasing proportion of litter-C in the mineral fraction. The more litter-C was associated with the mineral fraction at the end of the experiment the higher the final litter-C decomposition rates. One possible explanation for this unexpected result is that we fractionated the litter-C at the end of our incubation experiment, after the most labile OM had already been mineralized. If the particulate carbon is faster decomposed than the mineral-associated carbon, the size of the POM fraction would decrease more rapidly than that of the MAOM fraction. The more pronounced this difference in decomposability between MAOM and POM is, the larger will be the MAOM fraction relative to the POM fraction in the remaining carbon at the end of the long-term incubation. Conversely, we did not observe a positive correlation between mineral-associated permafrost-C and final permafrost-C decomposition rates, indicating that the two carbon sources (litter-C, permafrost-C) have different properties.

The strong positive correlation between MA-litter-C and MA-permafrost-C, and the absence of a correlation between the clay fraction and litter stabilization under oxic conditions indicates that mineral bound permafrost-C is more important for incorporating fresh plant litter into the mineral fraction than the size of the clay fraction itself. These results are supported by previous findings showing that fresh plant litter binds to pre-existing organo-mineral clusters rather than to the free surfaces of clay minerals (Vogel et al., 2014). The presence of C-pools with different degradability in the MAOM fraction has previously been proposed, for example based on the rapid incorporation of fresh plant litter into the MAOM fraction (Swanston et al., 2005). Kleber et al. (2007) proposed a model of organo-mineral interactions based on multiple layers, characterized by an inner contact zone between the mineral surface and OM with the highest strength of association, and an outer zone where OM is more loosely bound and can more easily be decomposed. This model aligns with our observations of a significantly lower MRT for litter-C compared to permafrost-C. Assuming that the decomposition products of added litter OM are bound to the outer layer of pre-existing permafrost OM mineral clusters, the litter C would be more readily available for microbial decomposition. This model could also explain why we found, contrary to our expectations, a positive correlation between litter-C decomposition parameters and the proportion of litter-C bound to the mineral fraction, which indicates that also relatively labile litter-C is present in the mineral-associated OM fraction.

https://doi.org/10.5194/egusphere-2025-6208
Preprint. Discussion started: 4 January 2026

Our study sheds new light and mechanistic understanding on the fate of fresh plant litter in thawing permafrost soils. However, the study was not designed to address some relevant in situ processes occurring on the landscape-scale, such as the dispersal of microbial communities into thawing permafrost (Monteux et al., 2020) or priming effects, although priming seems of minor importance in our permafrost samples (Knoblauch et al., 2018). We further cannot draw conclusions on the net carbon balance of Arctic landscapes based on our laboratory design, as this is affected by complex, nonlinear interactions between a variety of constantly changing environmental variables that cannot be simulated in a long-term laboratory experiment. For example, rising temperatures in the Arctic cause changes in vegetation composition and shrub expansion (Frost and Epstein, 2014). These shifts in vegetation alter the quantity and quality of litter entering the soil (Cornelissen et al., 2007), directly and indirectly affecting the landscape's carbon balance (Machmuller et al., 2024). Additionally, permafrost thaw leads to changes in landscape hydrology, particularly in ice-rich permafrost deposits such as those we studied, which affects the hydrological landscape connectivity, the composition of plant communities, the redox conditions in soils, and consequently the carbon balance of soils (Pegoraro et al., 2021; Jorgenson et al., 2022). However, we provide first evidence, that thawing permafrost not only contributes to the release of greenhouse gases after thaw but may also function as a long-term carbon sink for fresh plant litter. This mechanism is particularly relevant in hillslope abrupt thaw features, such as those observed at the Kurungnakh study site, where abrupt permafrost thaw causes the active layer to erode, exposing deep permafrost material to the surface within a short period of time. Such hillslope erosional features may become strong sources of greenhouse gases while they are active (Knoblauch et al., 2021; Cassidy et al., 2016; Mu et al., 2017) and contribute substantially to the greenhouse gas release form the permafrost zone (Turetsky et al., 2020). However, the regrowth of vegetation stabilizes these thaw features (Huebner et al., 2022), and may turn them from a carbon source into a carbon sink (Wickland et al., 2020).

5 Conclusions

The current study demonstrates that thawing permafrost is not only a source of organic carbon that may be decomposed to the greenhouse gases CO_2 and CH_4 but that thawing permafrost may also stabilize a substantial part of recent plant litter over decades mainly in the mineral associated fraction. By using stable isotope labelling and density fractionation we showed that the mean residence time of recent plant litter carbon is one order of magnitude lower than that of permafrost carbon, although a higher share of plant litter carbon was bound to the mineral fraction by the end of the experiment. Furthermore, we found no evidence that the proportion of particulate permafrost organic carbon in these mineral soils relates to the proportion of fast degradable, labile organic carbon. These results demonstrate that mineral-associated organic matter in thawing permafrost soils, which receive an input of fresh plant litter, contains organic matter with very different turnover times. Furthermore, the size of particulate organic matter in these mineral soils cannot be used as an indicator of fast-degradable, labile organic carbon. At least in case of permafrost organic matter, further parameters apart from mineral interactions contribute to organic matter stabilization. Our study emphasizes that the carbon balance of thawing permafrost soils depends not only on the release of old organic carbon from former permafrost, but also on its capacity to stabilize fresh organic matter resulting from increased plant

https://doi.org/10.5194/egusphere-2025-6208
Preprint. Discussion started: 4 January 2026

litter input due to higher primary productivity in a warmer Arctic. This is particularly relevant in landscapes affected by abrupt thaw features, where surface vegetation is eroded and deep permafrost is exposed, allowing new vegetation to establish over time and stabilize the soil surface. However, to decipher the carbon balance of thawing permafrost landscapes, a combination of field observations, complex laboratory experiments and process models is required, which consider the capacity of thawing permafrost to stabilize fresh plant litter.

Appendix

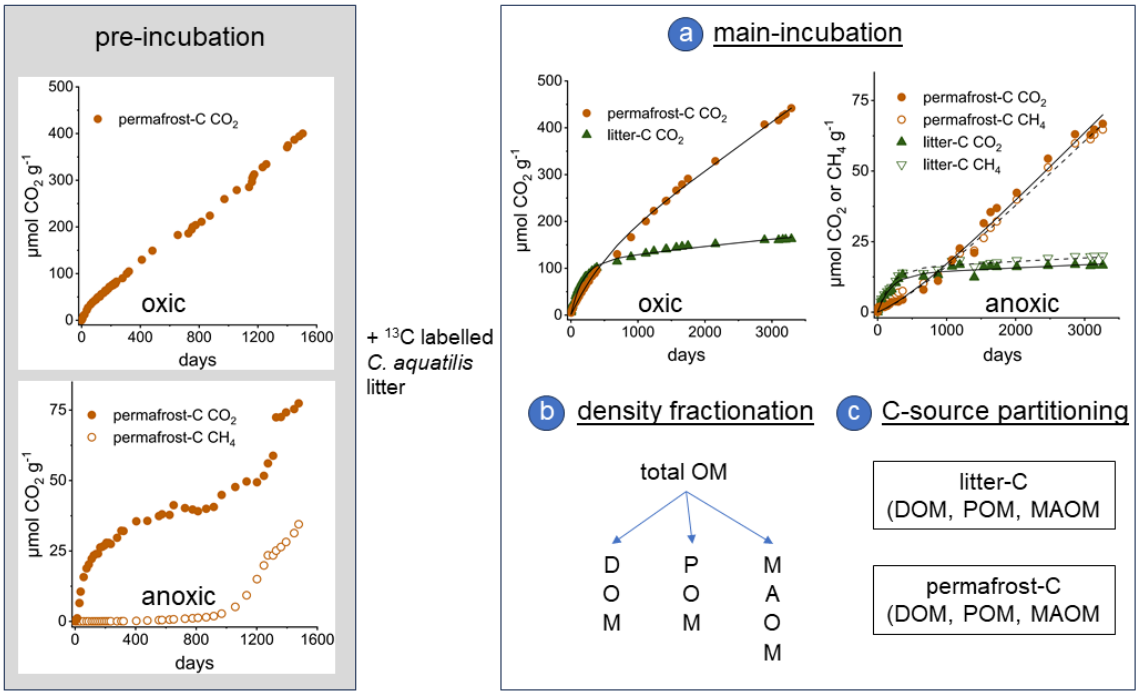

Figure A1: Timeline of the incubation experiment. Left panel: Pre-incubation of permafrost samples for four years under oxic and anoxic conditions at 4° C until constant CO_2 and CH_4 production rates have been established. Data of this pre-incubation experiment are not considered in this manuscript. At the end of the pre-incubation ^{13}C-labelled *Carex aquatilis* litter was added. Right panel: (a) Main incubation experiment. Cumulative CO_2 and CH_4 production under oxic and anoxic conditions from permafrost-C and litter-C in a permafrost sample from the Siberian Island Kurungnakh (0.9-1.1 m depth) incubated at 4° C for nine years. The left axis shows CO_2 and CH_4 produced from the two carbon sources (litter-C, permafrost-C). Black line represents the simulation of the calibrated two-pool carbon decomposition model for CO_2 (solid) and CH_4 (dashed). (b) Density fractionation of the organic carbon into the dissolved (DOM), the particulate (POM) and the mineral associated organic matter (MAOM) fraction at the end of the experiment. (c) Partitioning of the remaining carbon in the three fractions into the two different carbon sources (permafrost-C, litter-C) using the $\delta^{13}C$-signatures in the respective pools.

https://doi.org/10.5194/egusphere-2025-6208
Preprint. Discussion started: 4 January 2026

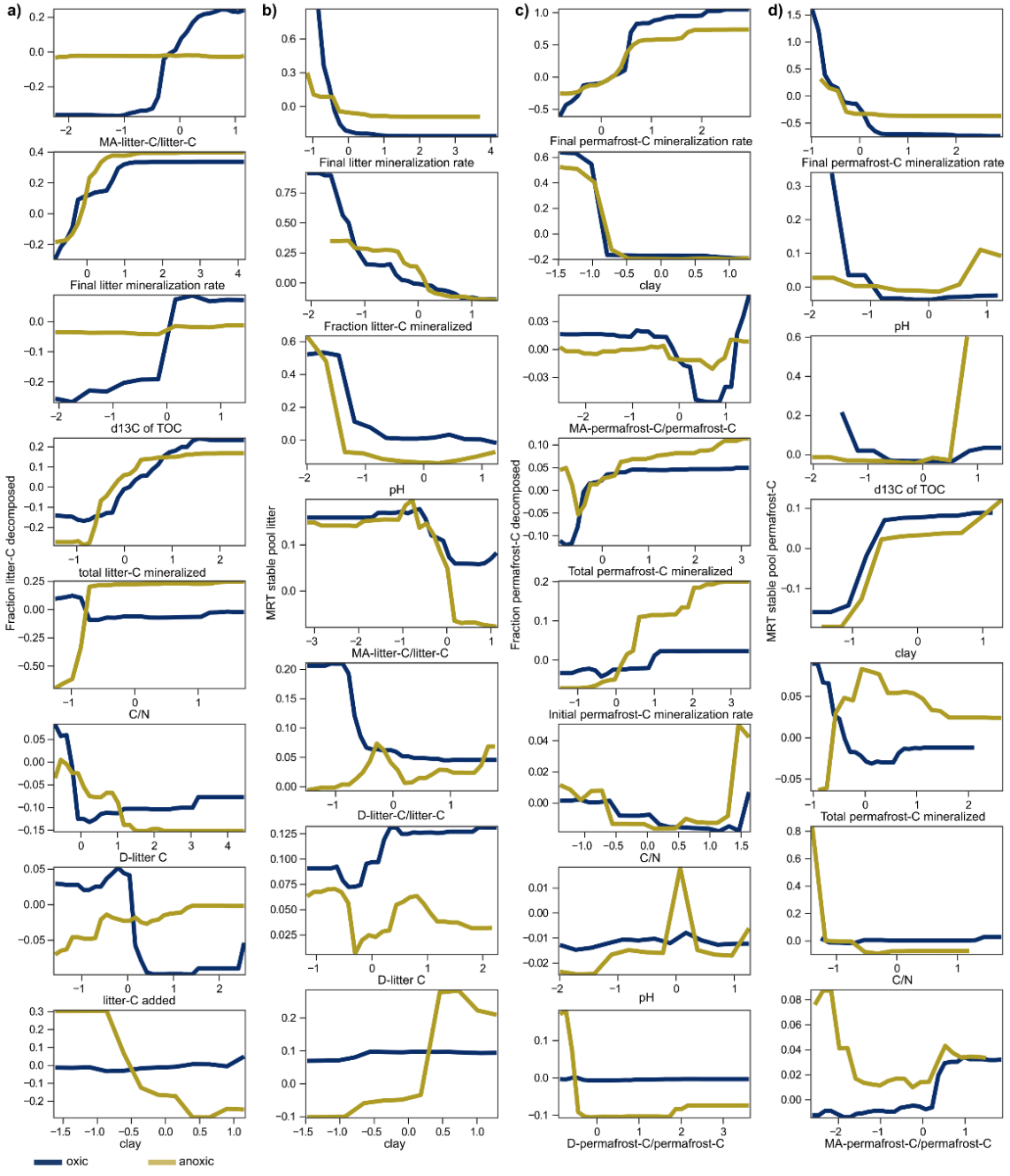

Figure A2: Partial dependence plots for Random Forest models, showing the responses of predictors used in Fig. 4. Panels show the fraction of litter-C decomposed (a), the mean residence time (MRT) of stable litter-C pool (b), the fraction of permafrost-C decomposed (c) and the MRT of the stable permafrost-C pool (d) under oxic and anoxic conditions. Note that variables were scaled prior to analyses using z-score centring.

https://doi.org/10.5194/egusphere-2025-6208
Preprint. Discussion started: 4 January 2026

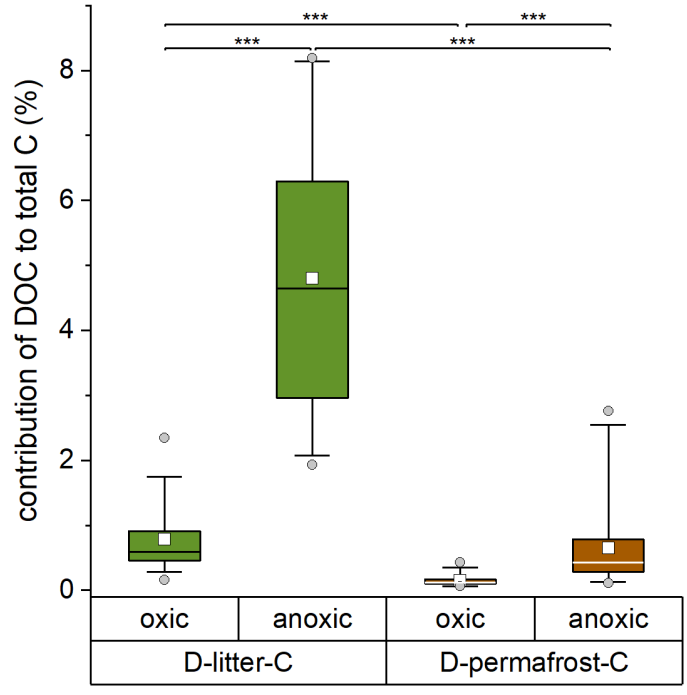

Figure A3: Contribution of the dissolved carbon fraction (DOC) to total litter-C and total permafrost-C recovered at the end of the experiment under oxic and anoxic incubation conditions. Significant differences are indicated by *** = p< 0.001 (Kruskal-Wallis ANOVA). The Box shows the 25/75 percentiles, the whiskers the 5/95 percentiles, the horizontal line the median and the white square the mean. Outliers are presented as circles.

https://doi.org/10.5194/egusphere-2025-6208
Preprint. Discussion started: 4 January 2026

Table A1: Characteristics of sampled permafrost deposits

site	depth	permafrost-C*	N*	C/N*	pH*	$\delta^{13}C$*	sand	silt	clay	litter-C added	
										oxic	anoxic
	m	mg g^{-1}	mg g^{-1}			‰ VPDB	%	%	%	mg C g^{-1}	mg C g^{-1}
Kurungnakh	0.66 - 0.78	38.1	2.0	19	4.0	-29.1	28.7	50.2	21.1	0.87	0.36
	0.86 - 1.10	121.0	7.8	16	4.8	-28.5	13.6	62.0	24.4	3.53	0.99
	1.16 - 1.29	72.0	4.8	15	4.3	-28.6	10.6	66.1	23.3	1.83	0.59
	3.84 - 4.04	36.7	2.9	12	6.9	-26.5	37.5	42.1	20.3	1.12	0.24
	4.34 - 4.54	47.0	3.5	13	7.2	-26.9	24.0	53.6	22.4	1.52	0.55
	3.34 - 3.54	33.9	2.7	13	7.2	-26.9	24.6	51.7	23.8	1.54	0.58
Samoylov	0.58 - 0.80	5.7	0.4	15	6.2	-27.3	85.2	11.9	2.9	0.30	0.15
	0.80 - 0.95	13.4	0.6	21	6.1	-27.0	78.0	17.2	4.8	0.51	0.21
	1.38 - 1.57	44.2	1.8	25	6.0	-25.9	53.6	38.6	7.8	1.87	0.71
	1.93 - 2.10	42.1	2.0	21	5.8	-27.4	49.9	40.6	9.5	1.64	0.68
	2.81 - 3.10	47.0	2.0	23	6.4	-26.6	46.1	40.8	13.1	1.37	0.53
	3.19 - 3.35	38.8	2.1	18	6.4	-26.6	36.7	52.8	10.5	1.84	0.56

*data from Knoblauch et al. (2018)

https://doi.org/10.5194/egusphere-2025-6208
Preprint. Discussion started: 4 January 2026

Table A2: Selected model parameters based on stepwise linear regression. Df = degrees of freedom, AIC=Akaike Information Criterion. For further analysis, models for aerobic and anaerobic samples were merged to include the same set of predictors, and due to the correlation between the different soil fractions, the clay fraction was included in all models to represent soil texture.

Model	dependent variable	treatment	independent variables	Df	AIC	Delta	Weight
Model A	fraction litter-C decomposed	oxic	C/N, final litter mineralization rate, litter-C added, MA-litter-C/litter-C, MRT stable litter-C pool, total litter-C mineralized	8	-11.4	0.74	0.104
Model B	MRT stable litter-C pool	oxic	clay, final litter mineralization rate, fraction litter-C mineralized, MA-litter-C/litter-C	6	55.5	1.90	0.071
Model C	fraction litter-C decomposed	anoxic	Clay, $\delta^{13}C$ of TOC, litter-C added, D-litter C, total litter-C mineralized	7	5.7	0.09	0.104
Model D	MRT stable litter-C pool	anoxic	D-litter-C/litter-C, fraction litter-C mineralized, D-litter C, pH	6	36.8	1.73	0.145
Model E	fraction permafrost-C decomposed	oxic	clay, C/N, D-permafrost-C/permafrost-C, final permafrost-C mineralization rate, initial permafrost-C mineralization rate, MA-permafrost-C/permafrost-C, N, pH, total permafrost-C mineralized	11	-46.8	0.25	0.139
Model F	MRT stable permafrost-C pool	oxic	clay, C/N, $\delta^{13}C$ of permafrost-C, final permafrost-C mineralization rate, fraction permafrost-C mineralized, pH, total permafrost-C mineralized	9	24.0	2.87	0.078
Model G	fraction permafrost-C decomposed	anoxic	final permafrost-C mineralization rate, initial permafrost-C mineralization rate, MA-permafrost-C/permafrost-C, N, total permafrost-C mineralized	7	-20.4	1.31	0.062
Model H	MRT stable permafrost-C pool	anoxic	clay, $\delta^{13}C$ of permafrost-C, MA- permafrost-C/permafrost-C, pH, total permafrost-C mineralized	7	4.0	1.58	0.162

https://doi.org/10.5194/egusphere-2025-6208
Preprint. Discussion started: 4 January 2026

Table A3: Fraction of total carbon decomposed during the first incubation year and final carbon decomposition rates standardized to the amount of carbon of the respective pool remaining at the end of the incubations.

Depth	Share of total litter-C decomposition in first year (%)		Share of total permafrost-C decomposition in first year (%)		Final litter-C decomposition rate (µmol C (mol litter-C)$^{-1}$d^{-1})		Final permafrost-C decomposition rate (µmol C (mol permafrost-C)$^{-1}$ d^{-1})	
(m)	oxic	anoxic	oxic	anoxic	oxic	anoxic	oxic	anoxic
Kurungnakh								
0.7-0.8	43.3±2.0	82.4±7.0	16.2±0.5	18.0±2.4	47.7±2.4	16.2±5.6	7.8±0.5	1.5±0.1
0.9-1.1	58.9±4.8	73.7±1.0	17.7±4.1	15.7±6.6	56.1±26.9	22.0±0.6	9.1±2.4	2.9±0.2
1.2-1.3	77.1±6.4	85.5±5.0	19.2±3.3	22.7±0.5	15.5±3.3	13.9±6.1	4.4±1.1	1.4±0.4
3.1-3.3	55.9±7.1	24.6±4.2	28.2±2.8	32.8±2.7	321±135	18.0±1.4	11.1±1.4	1.1±0.1
3.6-3.8	64.7±7.9	34.1±18.0	26.5±1.8	35.8±15.0	231±128	22.7±6.2	6.4±0.4	0.7±0.1
4.1-4.3	67.4±0.8	61.5±1.7	19.5±0.7	32.1±0.7	710±275	18.4±0.6	14.0±0.1	0.7±0.1
Samoylov								
0.6-0.8	47.9±1.3	77.1±2.8	11.7±1.0	14.7±2.5	220±35.5	41.3±6.1	48.7±7.0	9.7±2.6
0.8-1.0	51.1±9.7	71.8±0.7	9.1±0.7	13.1±1.4	225±90.1	42.8±3.7	43.3±0.5	7.3±0.3
1.4-1.6	53.1±3.2	68.5±2.3	16.3±1.5	12.0±1.3	177±34.6	64.2±18.6	24.6±2.9	6.5±2.7
1.9-2.1	41.7±2.5	81.4±3.0	15.4±1.7	18.5±2.6	107±7.6	23.6±4.3	17.7±3.4	2.2±0.1
2.8-3.1	81.8±4.9	79.6±0.7	18.7±2.2	24.4±1.3	76.3±19.5	12.3±0.3	10.3±2.3	0.9±0.1
3.2-3.4	65.2±3.1	82.2±4.4	22.7±2.0	21.5±1.7	81.2±37.6	21.5±3.1	11.0±1.5	1.4±0.1
Mean ± SD	59.7±13.3	69.4±19.4	18.8±5.7	21.3±9.4	192±21.4	27.4±17.0	16.9±13.9	3.2±3.3
Median (IQR)	61.4 (19.9)	74.4 (13.7)	18.6 (7.6)	21.5 (10.3)	131 (15.6)	21.8 (17.8)	12.4 (13.0)	1.6 (3.7)

Data Availability Statement

All data needed to evaluate the conclusions in the paper are present in the paper.

Author Contributions:

Christian Knoblauch: Conceptualization, Investigation, Methodology, Validation, Formal analysis, Writing – original draft – review & editing, Funding acquisition **Carolina Voigt:** Methodology, Formal analysis, Writing – review & editing **Christian Beer:** Conceptualization, Investigation, Methodology, Validation, Formal analysis, Writing – review & editing, Funding acquisition.

Competing interests

The authors declare no competing interests.

Acknowledgements

We thank R. Lendt and B. Grabellus for laboratory assistance and Carsten W. Mueller for valuable discussion.

https://doi.org/10.5194/egusphere-2025-6208
Preprint. Discussion started: 4 January 2026

Financial support

Support for this study was provided to C. Knoblauch by the German Research Foundation (DFG EXC 2037, CLICCS, 390683824), to C. Beer by the German Research Foundation Heisenberg-Program (DFG 508047523) and to C. Knoblauch and C. Voigt by the Federal Ministry of Research, Technology and Space (BMFTR MOMENT, 03F0931A).

References

Amundson, R. and Baisden, W. T.: Stable isotope tracers and mathematical models in soil organic matter studies, in: Methods in Ecosystem Science, edited by: Sala, O. E., Jackson, R. B., Mooney, H. A., and Howarth, R. B., Springer New York, 117-137, 2000.

Andrén, O. and Kätterer, T.: ICBM: The introductory carbon balance model for exploration of soil carbon balances, Ecol. Appl., 7, 1226-1236, http://dx.doi.org/10.2307/2641210, 1997.

Angst, G., Mueller, K. E., Nierop, K. G. J., and Simpson, M. J.: Plant- or microbial-derived? A review on the molecular composition of stabilized soil organic matter, Soil Biol. Biochem., 156, 108189, https://doi.org/10.1016/j.soilbio.2021.108189, 2021.

Arndt, K. A., Santos, M. J., Ustin, S., Davidson, S. J., Stow, D., Oechel, W. C., Tran, T. T. P., Graybill, B., and Zona, D.: Arctic greening associated with lengthening growing seasons in Northern Alaska, Environ. Res. Lett., 14, 125018, http://doi.org/10.1088/1748-9326/ab5e26, 2019.

Bartón, K.: MuMIn: Multi-Model Inference (R package version 1.47.5) [code], 2023.

Bastviken, D., Ejlertsson, J., and Tranvik, L.: Similar bacterial growth on dissolved organic matter in anoxic and oxic lake water, Aquat. Microb. Ecol., 24, 41-49, 2001.

Beer, C., Knoblauch, C., Hoyt, A. M., Hugelius, G., Palmtag, J., Mueller, C. W., and Trumbore, S.: Vertical pattern of organic matter decomposability in cryoturbated permafrost-affected soils, Environ. Res. Lett., 17, 104023, http://doi.org/10.1088/1748-9326/ac9198, 2022.

Begill, N., Don, A., and Poeplau, C.: No detectable upper limit of mineral-associated organic carbon in temperate agricultural soils, Global Change Biology, 29, 4662-4669, https://doi.org/10.1111/gcb.16804, 2023.

Belshe, E. F., Schuur, E. A. G., and Bolker, B. M.: Tundra ecosystems observed to be CO_2 sources due to differential amplification of the carbon cycle, Ecol. Lett., 16, 1307-1315, http://dx.doi.org/10.1111/ele.12164, 2013.

Berner, L. T., Massey, R., Jantz, P., Forbes, B. C., Macias-Fauria, M., Myers-Smith, I., Kumpula, T., Gauthier, G., Andreu-Hayles, L., Gaglioti, B. V., Burns, P., Zetterberg, P., D'Arrigo, R., and Goetz, S. J.: Summer warming explains widespread but not uniform greening in the Arctic tundra biome, Nat. Commun., 11, 4621, http://doi.org/10.1038/s41467-020-18479-5, 2020.

Bischoff, J., Mangelsdorf, K., Gattinger, A., Schloter, M., Kurchatova, A. N., Herzschuh, U., and Wagner, D.: Response of methanogenic archaea to Late Pleistocene and Holocene climate changes in the Siberian Arctic, Global Biogeochem. Cy., 27, 305-317, http://doi.org/10.1029/2011GB004238, 2013.

Bonanomi, G., Incerti, G., Giannino, F., Mingo, A., Lanzotti, V., and Mazzoleni, S.: Litter quality assessed by solid state 13C NMR spectroscopy predicts decay rate better than C/N and Lignin/N ratios, Soil Biol. Biochem., 56, 40-48, https://doi.org/10.1016/j.soilbio.2012.03.003, 2013.

Breiman, L.: Random forests, Machine Learning, 45, 5-32, 2001.

Bridgham, S. D., Updegraff, K., and Pastor, J.: Carbon, nitrogen, and phosphorus mineralization in northern wetlands, Ecology, 79, 1545-1561, 1998.

Carvalhais, N., Forkel, M., Khomik, M., Bellarby, J., Jung, M., Migliavacca, M., Mu, M., Saatchi, S., Santoro, M., Thurner, M., Weber, U., Ahrens, B., Beer, C., Cescatti, A., Randerson, J. T., and Reichstein, M.: Global covariation of carbon turnover times with climate in terrestrial ecosystems, Nature, 514, 213-217, https://doi.org/10.1038/nature13731, 2014.

Cassidy, A. E., Christen, A., and Henry, G. H. R.: The effect of a permafrost disturbance on growing-season carbon-dioxide fluxes in a high Arctic tundra ecosystem, Biogeosciences, 13, 2291-2303, http://doi.org/10.5194/bg-13-2291-2016, 2016.

https://doi.org/10.5194/egusphere-2025-6208
Preprint. Discussion started: 4 January 2026

Cerli, C., Celi, L., Kalbitz, K., Guggenberger, G., and Kaiser, K.: Separation of light and heavy organic matter fractions in soil — Testing for proper density cut-off and dispersion level, Geoderma, 170, 403-416, https://doi.org/10.1016/j.geoderma.2011.10.009, 2012.

Cheng, X., Xing, W., and Liu, J.: Litter chemical traits, microbial and soil stoichiometry regulate organic carbon accrual of particulate and mineral-associated organic matter, Biol. Fert. Soils, 59, 777-790, http://doi.org/10.1007/s00374-023-01746-0, 2023.

Cornelissen, J. H. C., Van Bodegom, P. M., Aerts, R., Callaghan, T. V., Van Logtestijn, R. S. P., Alatalo, J., Stuart Chapin, F., Gerdol, R., Gudmundsson, J., Gwynn-Jones, D., Hartley, A. E., Hik, D. S., Hofgaard, A., Jónsdóttir, I. S., Karlsson, S., Klein, J. A., Laundre, J., Magnusson, B., Michelsen, A., Molau, U., Onipchenko, V. G., Quested, H. M., Sandvik, S. M., Schmidt, I. K., Shaver, G. R., Solheim, B., Soudzilovskaia, N. A., Stenström, A., Tolvanen, A., Totland, Ø., Wada, N., Welker, J. M., Zhao, X., and Team, M. O. L.: Global negative vegetation feedback to climate warming responses of leaf litter decomposition rates in cold biomes, Ecol. Lett., 10, 619-627, https://doi.org/10.1111/j.1461-0248.2007.01051.x, 2007.

Cotrufo, M. F., Wallenstein, M. D., Boot, C. M., Denef, K., and Paul, E.: The Microbial Efficiency-Matrix Stabilization (MEMS) framework integrates plant litter decomposition with soil organic matter stabilization: do labile plant inputs form stable soil organic matter?, Global Change Biology, 19, 988-995, https://doi.org/10.1111/gcb.12113, 2013.

Drake, T. W., Wickland, K. P., Spencer, R. G. M., McKnight, D. M., and Striegl, R. G.: Ancient low–molecular-weight organic acids in permafrost fuel rapid carbon dioxide production upon thaw, Proceedings of the National Academy of Sciences, 112, 13946-13951, http://doi.org/10.1073/pnas.1511705112, 2015.

Eckhardt, T., Knoblauch, C., Kutzbach, L., Holl, D., Simpson, G., Abakumov, E., and Pfeiffer, E.-M.: Partitioning net ecosystem exchange of CO_2 on the pedon scale in the Lena River Delta, Siberia, Biogeosciences, 16, 1543-1562, http://doi.org/10.5194/bg-16-1543-2019, 2019.

Elberling, B., Michelsen, A., Schädel, C., Schuur, E. A. G., Christiansen, H. H., Berg, L., Tamstorf, M. P., and Sigsgaard, C.: Long-term CO_2 production following permafrost thaw, Nat. Clim. Change, 3, 890-894, http://doi.org/10.1038/nclimate1955, 2013.

Elmendorf, S. C., Henry, G. H. R., Hollister, R. D., Björk, R. G., Boulanger-Lapointe, N., Cooper, E. J., Cornelissen, J. H. C., Day, T. A., Dorrepaal, E., Elumeeva, T. G., Gill, M., Gould, W. A., Harte, J., Hik, D. S., Hofgaard, A., Johnson, D. R., Johnstone, J. F., Jónsdóttir, I. S., Jorgenson, J. C., Klanderud, K., Klein, J. A., Koh, S., Kudo, G., Lara, M., Lévesque, E., Magnússon, B., May, J. L., Mercado-Dı´az, J. A., Michelsen, A., Molau, U., Myers-Smith, I. H., Oberbauer, S. F., Onipchenko, V. G., Rixen, C., Martin Schmidt, N., Shaver, G. R., Spasojevic, M. J., Þórhallsdóttir, Þ. E., Tolvanen, A., Troxler, T., Tweedie, C. E., Villareal, S., Wahren, C.-H., Walker, X., Webber, P. J., Welker, J. M., and Wipf, S.: Plot-scale evidence of tundra vegetation change and links to recent summer warming, Nat. Clim. Change, 2, 453-457, https://doi.org/10.1038/nclimate1465, 2012.

Euskirchen, E. S., McGuire, A. D., Kicklighter, D. W., Zhuang, Q., Clein, J. S., Dargaville, R. J., Dye, D. G., Kimball, J. S., McDonald, K. C., Melillo, J. M., Romanovsky, V. E., and Smith, N. V.: Importance of recent shifts in soil thermal dynamics on growing season length, productivity, and carbon sequestration in terrestrial high-latitude ecosystems, Global Change Biology, 12, 731-750, https://doi.org/10.1111/j.1365-2486.2006.01113.x, 2006.

Faucherre, S., Jørgensen, C. J., Blok, D., Weiss, N., Siewert, M. B., Bang-Andreasen, T., Hugelius, G., Kuhry, P., and Elberling, B.: Short and long-term controls on active layer and permafrost carbon turnover across the Arctic, J. Geophys. Res. Biogeo., 123, 372-390, http://doi.org/10.1002/2017JG004069, 2018.

Freeman, C., Ostle, N., and Kang, H.: An enzymic 'latch' on a global carbon store, Nature, 409, 149-149, 2001.

Frost, G. V. and Epstein, H. E.: Tall shrub and tree expansion in Siberian tundra ecotones since the 1960s, Global Change Biology, 20, 1264-1277, http://doi.org/10.1111/gcb.12406, 2014.

García-Palacios, P., Bradford, M. A., Benavente-Ferraces, I., de Celis, M., Delgado-Baquerizo, M., García-Gil, J. C., Gaitán, J. J., Goñi-Urtiaga, A., Mueller, C. W., Panettieri, M., Rey, A., Sáez-Sandino, T., Schuur, E. A. G., Sokol, N. W., Tedersoo, L., and Plaza, C.: Dominance of particulate organic carbon in top mineral soils in cold regions, Nat. Geosci., 17, 145-150, http://doi.org/10.1038/s41561-023-01354-5, 2024.

Gentsch, N., Mikutta, R., Shibistova, O., Wild, B., Schnecker, J., Richter, A., Urich, T., Gittel, A., Santruckova, H., Barta, J., Lashchinskiy, N., Mueller, C. W., Fuss, R., and Guggenberger, G.: Properties and bioavailability of particulate and mineral-associated organic matter in Arctic permafrost soils, Lower Kolyma Region, Russia, Eur. J. Soil Sci., 66, 722-734, http://doi.org/10.1111/ejss.12269, 2015a.

https://doi.org/10.5194/egusphere-2025-6208
Preprint. Discussion started: 4 January 2026

Gentsch, N., Mikutta, R., Alves, R. J. E., Barta, J., Čapek, P., Gittel, A., Hugelius, G., Kuhry, P., Lashchinskiy, N., Palmtag, J., Richter, A., Šantrůčková, H., Schnecker, J., Shibistova, O., Urich, T., Wild, B., and Guggenberger, G.: Storage and transformation of organic matter fractions in cryoturbated permafrost soils across the Siberian Arctic, Biogeosciences, 12, 4525-4542, http://doi.org/10.5194/bg-12-4525-2015, 2015b.

Gentsch, N., Wild, B., Mikutta, R., Čapek, P., Diáková, K., Schrumpf, M., Turner, S., Minnich, C., Schaarschmidt, F., Shibistova, O., Schnecker, J., Urich, T., Gittel, A., Šantrůčková, H., Bárta, J., Lashchinskiy, N., Fuß, R., Richter, A., and Guggenberger, G.: Temperature response of permafrost soil carbon is attenuated by mineral protection, Global Change Biology, 24, 3401–3415, http://doi.org/10.1111/gcb.14316, 2018.

Guo, Y.-X., Yu, G.-H., Hu, S., Liang, C., Kappler, A., Jorgenson, Mark T., Guo, L., and Guggenberger, G.: Deciphering the intricate control of minerals on deep soil carbon stability and persistence in Alaskan permafrost, Global Change Biology, 30, e17552, https://doi.org/10.1111/gcb.17552, 2024.

Haddix, M. L., Paul, E. A., and Cotrufo, M. F.: Dual, differential isotope labeling shows the preferential movement of labile plant constituents into mineral-bonded soil organic matter, Global Change Biology, 22, 2301-2312, https://doi.org/10.1111/gcb.13237, 2016.

Haddix, M. L., Gregorich, E. G., Helgason, B. L., Janzen, H., Ellert, B. H., and Francesca Cotrufo, M.: Climate, carbon content, and soil texture control the independent formation and persistence of particulate and mineral-associated organic matter in soil, Geoderma, 363, 114160, https://doi.org/10.1016/j.geoderma.2019.114160, 2020.

Heckman, K., Hicks Pries, C. E., Lawrence, C. R., Rasmussen, C., Crow, S. E., Hoyt, A. M., von Fromm, S. F., Shi, Z., Stoner, S., McGrath, C., Beem-Miller, J., Berhe, A. A., Blankinship, J. C., Keiluweit, M., Marín-Spiotta, E., Monroe, J. G., Plante, A. F., Schimel, J., Sierra, C. A., Thompson, A., and Wagai, R.: Beyond bulk: Density fractions explain heterogeneity in global soil carbon abundance and persistence, Global Change Biology, 28, 1178-1196, https://doi.org/10.1111/gcb.16023, 2022.

Heikkinen, J. E. P., Elsakov, V., and Martikainen, P. J.: Carbon dioxide and methane dynamics and annual carbon balance in tundra wetland in NE Europe, Russia, Global Biogeochem. Cy., 16, 1115, https://doi.org/10.1029/2002gb001930, 2002.

Huebner, D. C., Buchwal, A., and Bret-Harte, M. S.: Retrogressive thaw slumps in the Alaskan Low Arctic may influence tundra shrub growth more strongly than climate, Ecosphere, 13, e4106, https://doi.org/10.1002/ecs2.4106, 2022.

Hugelius, G., Strauss, J., Zubrzycki, S., Harden, J. W., Schuur, E. A. G., Ping, C.-L., Schirrmeister, L., Grosse, G., Michaelson, G. J., Koven, C. D., O'Donnell, J. A., Elberling, B., Mishra, U., Camill, P., Yu, Z., Palmtag, J., and Kuhry, P.: Estimated stocks of circumpolar permafrost carbon with quantified uncertainty ranges and identified data gaps, Biogeosciences, 11, 6573-6593, http://doi.org/10.5194/bg-11-6573-2014, 2014.

Hugelius, G., Ramage, J., Burke, E., Chatterjee, A., Smallman, T. L., Aalto, T., Bastos, A., Biasi, C., Canadell, J. G., Chandra, N., Chevallier, F., Ciais, P., Chang, J., Feng, L., Jones, M. W., Kleinen, T., Kuhn, M., Lauerwald, R., Liu, J., López-Blanco, E., Luijkx, I. T., Marushchak, M. E., Natali, S. M., Niwa, Y., Olefeldt, D., Palmer, P. I., Patra, P. K., Peters, W., Potter, S., Poulter, B., Rogers, B. M., Riley, W. J., Saunois, M., Schuur, E. A. G., Thompson, R. L., Treat, C., Tsuruta, A., Turetsky, M. R., Virkkala, A. M., Voigt, C., Watts, J., Zhu, Q., and Zheng, B.: Permafrost region greenhouse gas budgets suggest a weak CO_2 sink and CH_4 and N_2O sources, but magnitudes differ between top-down and bottom-up methods, Global Biogeochem. Cy., 38, e2023GB007969, https://doi.org/10.1029/2023GB007969, 2024.

ISO 11277: Soil quality — Determination of particle size distribution in mineral soil material — Method by sieving and sedimentation, 2002.

Jagadamma, S., Steinweg, J. M., Mayes, M. A., Wang, G., and Post, W. M.: Decomposition of added and native organic carbon from physically separated fractions of diverse soils, Biol. Fert. Soils, 50, 613-621, http://doi.org/10.1007/s00374-013-0879-2, 2014.

Jorgenson, M. T., Kanevskiy, M. Z., Jorgenson, J. C., Liljedahl, A., Shur, Y., Epstein, H., Kent, K., Griffin, C. G., Daanen, R., Boldenow, M., Orndahl, K., Witharana, C., and Jones, B. M.: Rapid transformation of tundra ecosystems from ice-wedge degradation, Global Planet. Change, 216, 103921, https://doi.org/10.1016/j.gloplacha.2022.103921, 2022.

Kaiser, C., Meyer, H., Biasi, C., Rusalimova, O., Barsukov, P., and Richter, A.: Conservation of soil organic matter through cryoturbation in arctic soils in Siberia, J. Geophys. Res. Biogeo., 112, G02017, 10.1029/2006JG000258, 2007.

Kleber, M., Sollins, P., and Sutton, R.: A conceptual model of organo-mineral interactions in soils: self-assembly of organic molecular fragments into zonal structures on mineral surfaces, Biogeochemistry, 85, 9-24, https://doi.org/10.1007/s10533-007-9103-5, 2007.

https://doi.org/10.5194/egusphere-2025-6208
Preprint. Discussion started: 4 January 2026

Knoblauch, C., Beer, C., Liebner, S., Grigoriev, M. N., and Pfeiffer, E.-M.: Methane production as key to the greenhouse gas budget of thawing permafrost, Nat. Clim. Change, 8, 309-312, http://doi.org/10.1038/s41558-018-0095-z, 2018.

Knoblauch, C., Beer, C., Sosnin, A., Wagner, D., and Pfeiffer, E.-M.: Predicting long-term carbon mineralization and trace gas production from thawing permafrost of Northeast Siberia, Global Change Biology, 19, 1160-1172, http://doi.org/10.1111/gcb.12116, 2013.

Knoblauch, C., Beer, C., Schuett, A., Sauerland, L., Liebner, S., Steinhof, A., Rethemeyer, J., Grigoriev, M. N., Faguet, A., and Pfeiffer, E.-M.: Carbon dioxide and methane release following abrupt thaw of Pleistocene permafrost deposits in Arctic Siberia, J. Geophys. Res. Biogeo., 126, e2021JG006543, https://doi.org/10.1029/2021JG006543, 2021.

Köchy, M., Hiederer, R., and Freibauer, A.: Global distribution of soil organic carbon – Part 1: Masses and frequency distributions of SOC stocks for the tropics, permafrost regions, wetlands, and the world, SOIL, 1, 351-365, http://doi.org/10.5194/soil-1-351-2015, 2015.

Kögel-Knabner, I., Guggenberger, G., Kleber, M., Kandeler, E., Kalbitz, K., Scheu, S., Eusterhues, K., and Leinweber, P.: Organo-mineral associations in temperate soils: Integrating biology, mineralogy, and organic matter chemistry, J. Plant Nutr. Soil Sci., 171, 61-82, https://doi.org/10.1002/jpln.200700048, 2008.

Kuhry, P. and Vitt, D. H.: Fossil carbon/nitrogen ratios as a measure of peat decomposition, Ecology, 77, 271-275, https://doi.org/10.2307/2265676, 1996.

Kutzbach, L., Wagner, D., and Pfeiffer, E.-M.: Effect of microrelief and vegetation on methane emission from wet polygonal tundra, Lena Delta, Northern Siberia, Biogeochemistry, 69, 341-362, 2004.

LaRowe, D. E. and Van Cappellen, P.: Degradation of natural organic matter: A thermodynamic analysis, Geochim. Cosmochim. Ac., 75, 2030-2042, https://doi.org/10.1016/j.gca.2011.01.020, 2011.

Lashchinskiy, N. N., Kartoziia, A. A., and Faguet, A. N.: Permafrost degradation as a supporting factor for the biodiversity of tundra ecosystems, Contemporary Problems of Ecology, 13, 401-411, http://doi.org/10.1134/S1995425520040071, 2020.

Lewkowicz, A. G. and Way, R. G.: Extremes of summer climate trigger thousands of thermokarst landslides in a High Arctic environment, Nat. Commun., 10, 1329, http://doi.org/10.1038/s41467-019-09314-7, 2019.

Lin, Y., Campbell, A. N., Bhattacharyya, A., DiDonato, N., Thompson, A. M., Tfaily, M. M., Nico, P. S., Silver, W. L., and Pett-Ridge, J.: Differential effects of redox conditions on the decomposition of litter and soil organic matter, Biogeochemistry, 154, 1-15, http://doi.org/10.1007/s10533-021-00790-y, 2021.

Louppe, G., Wehenkel, L., Sutera, A., and Geurts, P.: Understanding variable importances in forests of randomized trees, in: Advances in Neural Information Processing Systems, edited by: Burges, C. J., Bottou, L., Welling, M., Ghahramani, Z., and Weinberger, K. Q., 2013.

Machmuller, M. B., Lynch, L. M., Mosier, S. L., Shaver, G. R., Calderon, F., Gough, L., Haddix, M. L., McLaren, J. R., Paul, E. A., Weintraub, M. N., Cotrufo, M. F., and Wallenstein, M. D.: Arctic soil carbon trajectories shaped by plant–microbe interactions, Nat. Clim. Change, 14, 1178-1185, http://doi.org/10.1038/s41558-024-02147-3, 2024.

Marschner, B., Brodowski, S., Dreves, A., Gleixner, G., Gude, A., Grootes, P. M., Hamer, U., Heim, A., Jandl, G., Ji, R., Kaiser, K., Kalbitz, K., Kramer, C., Leinweber, P., Rethemeyer, J., Schaeffer, A., Schmidt, M. W. I., Schwark, L., and Wiesenberg, G. L. B.: How relevant is recalcitrance for the stabilization of organic matter in soils?, J. Plant Nutr. Soil Sci., 171, 91-110, https://doi.org/10.1002/jpln.200700049, 2008.

Martens, J., Mueller, C. W., Joshi, P., Rosinger, C., Maisch, M., Kappler, A., Bonkowski, M., Schwamborn, G., Schirrmeister, L., and Rethemeyer, J.: Stabilization of mineral-associated organic carbon in Pleistocene permafrost, Nat. Commun., 14, 2120, http://doi.org/10.1038/s41467-023-37766-5, 2023.

Mikan, C. J., Schimel, J. P., and Doyle, A. P.: Temperature controls of microbial respiration in arctic tundra soils above and below freezing, Soil Biol. Biochem., 34, 1785-1795, 2002.

Monteux, S., Keuper, F., Fontaine, S., Gavazov, K., Hallin, S., Juhanson, J., Krab, E. J., Revaillot, S., Verbruggen, E., Walz, J., Weedon, J. T., and Dorrepaal, E.: Carbon and nitrogen cycling in Yedoma permafrost controlled by microbial functional limitations, Nat. Geosci., 13, 794-798, http://doi.org/10.1038/s41561-020-00662-4, 2020.

Mu, C. C., Abbott, B. W., Zhao, Q., Su, H., Wang, S. F., Wu, Q. B., Zhang, T. J., and Wu, X. D.: Permafrost collapse shifts alpine tundra to a carbon source but reduces N_2O and CH_4 release on the northern Qinghai-Tibetan Plateau, Geophys. Res. Lett., 44, 8945-8952, http://doi.org/10.1002/2017gl074338, 2017.

https://doi.org/10.5194/egusphere-2025-6208
Preprint. Discussion started: 4 January 2026

Mueller, C. W., Rethemeyer, J., Kao-Kniffin, J., Löppmann, S., Hinkel, K. M., and G. Bockheim, J.: Large amounts of labile organic carbon in permafrost soils of northern Alaska, Global Change Biology, 21, 2804-2817, http://doi.org/10.1111/gcb.12876, 2015.

Natali, S. M., Schuur, E. A. G., and Rubin, R. L.: Increased plant productivity in Alaskan tundra as a result of experimental warming of soil and permafrost, J. Ecol., 100, 488-498, https://doi.org/10.1111/j.1365-2745.2011.01925.x, 2012.

Natali, S. M., Watts, J. D., Rogers, B. M., Potter, S., Ludwig, S. M., Selbmann, A.-K., Sullivan, P. F., Abbott, B. W., Arndt, K. A., Birch, L., Björkman, M. P., Bloom, A. A., Celis, G., Christensen, T. R., Christiansen, C. T., Commane, R., Cooper, E. J., Crill, P., Czimczik, C., Davydov, S., Du, J., Egan, J. E., Elberling, B., Euskirchen, E. S., Friborg, T., Genet, H., Göckede, M., Goodrich, J. P., Grogan, P., Helbig, M., Jafarov, E. E., Jastrow, J. D., Kalhori, A. A. M., Kim, Y., Kimball, J. S., Kutzbach, L., Lara, M. J., Larsen, K. S., Lee, B.-Y., Liu, Z., Loranty, M. M., Lund, M., Lupascu, M., Madani, N., Malhotra, A., Matamala, R., McFarland, J., McGuire, A. D., Michelsen, A., Minions, C., Oechel, W. C., Olefeldt, D., Parmentier, F.-J. W., Pirk, N., Poulter, B., Quinton, W., Rezanezhad, F., Risk, D., Sachs, T., Schaefer, K., Schmidt, N. M., Schuur, E. A. G., Semenchuk, P. R., Shaver, G., Sonnentag, O., Starr, G., Treat, C. C., Waldrop, M. P., Wang, Y., Welker, J., Wille, C., Xu, X., Zhang, Z., Zhuang, Q., and Zona, D.: Large loss of CO_2 in winter observed across the northern permafrost region, Nat. Clim. Change, 9, 852-857, http://doi.org/10.1038/s41558-019-0592-8, 2019.

Obu, J., Westermann, S., Bartsch, A., Berdnikov, N., Christiansen, H. H., Dashtseren, A., Delaloye, R., Elberling, B., Etzelmüller, B., Kholodov, A., Khomutov, A., Kääb, A., Leibman, M. O., Lewkowicz, A. G., Panda, S. K., Romanovsky, V., Way, R. G., Westergaard-Nielsen, A., Wu, T., Yamkhin, J., and Zou, D.: Northern Hemisphere permafrost map based on TTOP modelling for 2000–2016 at 1 km^2 scale, Earth-Sci. Rev., 193, 299-316, https://doi.org/10.1016/j.earscirev.2019.04.023, 2019.

Patzner, M. S., Mueller, C. W., Malusova, M., Baur, M., Nikeleit, V., Scholten, T., Hoeschen, C., Byrne, J. M., Borch, T., Kappler, A., and Bryce, C.: Iron mineral dissolution releases iron and associated organic carbon during permafrost thaw, Nat. Commun., 11, 6329, http://doi.org/10.1038/s41467-020-20102-6, 2020.

Pegoraro, E. F., Mauritz, M. E., Ogle, K., Ebert, C. H., and Schuur, E. A. G.: Lower soil moisture and deep soil temperatures in thermokarst features increase old soil carbon loss after 10 years of experimental permafrost warming, Global Change Biology, 27, 1293-1308, http://doi.org/10.1111/gcb.15481, 2021.

Ping, C. L., Jastrow, J. D., Jorgenson, M. T., Michaelson, G. J., and Shur, Y. L.: Permafrost soils and carbon cycling, SOIL, 1, 147-171, http://doi.org/10.5194/soil-1-147-2015, 2015.

Prater, I., Zubrzycki, S., Buegger, F., Zoor-Füllgraff, L. C., Angst, G., Dannenmann, M., and Mueller, C. W.: From fibrous plant residues to mineral-associated organic carbon – the fate of organic matter in Arctic permafrost soils, Biogeosciences, 17, 3367–3383, http://doi.org/10.5194/bg-17-3367-2020, 2020.

Qin, S., Zhang, D., Wei, B., and Yang, Y.: Dual roles of microbes in mediating soil carbon dynamics in response to warming, Nat. Commun., 15, 6439, 10.1038/s41467-024-50800-4, 2024.

Qin, S., Kou, D., Mao, C., Chen, Y., Chen, L., and Yang, Y.: Temperature sensitivity of permafrost carbon release mediated by mineral and microbial properties, Sci. Adv., 7, eabe3596, http://doi.org/10.1126/sciadv.abe3596, 2021.

Rantanen, M., Karpechko, A. Y., Lipponen, A., Nordling, K., Hyvärinen, O., Ruosteenoja, K., Vihma, T., and Laaksonen, A.: The Arctic has warmed nearly four times faster than the globe since 1979, Communications Earth & Environment, 3, 168, http://doi.org/10.1038/s43247-022-00498-3, 2022.

Schädel, C., Schuur, E. A. G., Bracho, R., Elberling, B., Knoblauch, C., Lee, H., Luo, Y., Shaver, G. R., and Turetsky, M. R.: Circumpolar assessment of permafrost C quality and its vulnerability over time using long-term incubation data, Global Change Biology, 20, 641-652, http://doi.org/10.1111/gcb.12417, 2014.

Schädel, C., Bader, M. K. F., Schuur, E. A. G., Biasi, C., Bracho, R., Capek, P., De Baets, S., Diakova, K., Ernakovich, J., Estop-Aragones, C., Graham, D. E., Hartley, I. P., Iversen, C. M., Kane, E., Knoblauch, C., Lupascu, M., Martikainen, P. J., Natali, S. M., Norby, R. J., O'Donnell, J. A., Chowdhury, T. R., Santruckova, H., Shaver, G., Sloan, V. L., Treat, C. C., Turetsky, M. R., Waldrop, M. P., and Wickland, K. P.: Potential carbon emissions dominated by carbon dioxide from thawed permafrost soils, Nat. Clim. Change, 6, 950-953, http://doi.org/10.1038/nclimate3054, 2016.

Schmidt, M. W. I., Torn, M. S., Abiven, S., Dittmar, T., Guggenberger, G., Janssens, I. A., Kleber, M., Kögel-Knabner, I., Lehmann, J., Manning, D. A. C., Nannipieri, P., Rasse, D. P., Weiner, S., and Trumbore, S. E.: Persistence of soil organic matter as an ecosystem property, Nature, 478, 49-56, 2011.

https://doi.org/10.5194/egusphere-2025-6208
Preprint. Discussion started: 4 January 2026

Schrumpf, M., Kaiser, K., Guggenberger, G., Persson, T., Kögel-Knabner, I., and Schulze, E.-D.: Storage and stability of organic carbon in soils as related to depth, occlusion within aggregates, and attachment to minerals, Biogeosciences, 10, 1675–1691, http://doi.org/10.5194/bg-10-1675-2013, 2013.

Sinsabaugh, R. L.: Phenol oxidase, peroxidase and organic matter dynamics of soil, Soil Biol. Biochem., 42, 391-404, https://doi.org/10.1016/j.soilbio.2009.10.014, 2010.

Swanston, C. W., Torn, M. S., Hanson, P. J., Southon, J. R., Garten, C. T., Hanlon, E. M., and Ganio, L.: Initial characterization of processes of soil carbon stabilization using forest stand-level radiocarbon enrichment, Geoderma, 128, 52-62, https://doi.org/10.1016/j.geoderma.2004.12.015, 2005.

Torn, M. S., Kleber, M., Zavaleta, E. S., Zhu, B., Field, C. B., and Trumbore, S. E.: A dual isotope approach to isolate soil carbon pools of different turnover times, Biogeosciences, 10, 8067-8081, http://doi.org/10.5194/bg-10-8067-2013, 2013.

Tuomi, M., Thum, T., Jarvinen, H., Fronzek, S., Berg, B., Harmon, M., Trofymow, J. A., Sevanto, S., and Liski, J.: Leaf litter decomposition-Estimates of global variability based on Yasso07 model, Ecol. Model., 220, 3362-3371, https://doi.org/10.1016/j.ecolmodel.2009.05.016, 2009.

Turetsky, M. R., Abbott, B. W., Jones, M. C., Anthony, K. W., Olefeldt, D., Schuur, E. A. G., Grosse, G., Kuhry, P., Hugelius, G., Koven, C., Lawrence, D. M., Gibson, C., Sannel, A. B. K., and McGuire, A. D.: Carbon release through abrupt permafrost thaw, Nat. Geosci., 13, 138-143, http://doi.org/10.1038/s41561-019-0526-0, 2020.

Virkkala, A.-M., Aalto, J., Rogers, B. M., Tagesson, T., Treat, C. C., Natali, S. M., Watts, J. D., Potter, S., Lehtonen, A., Mauritz, M., Schuur, E. A. G., Kochendorfer, J., Zona, D., Oechel, W., Kobayashi, H., Humphreys, E., Goeckede, M., Iwata, H., Lafleur, P. M., Euskirchen, E. S., Bokhorst, S., Marushchak, M., Martikainen, P. J., Elberling, B., Voigt, C., Biasi, C., Sonnentag, O., Parmentier, F.-J. W., Ueyama, M., Celis, G., St.Louis, V. L., Emmerton, C. A., Peichl, M., Chi, J., Järveoja, J., Nilsson, M. B., Oberbauer, S. F., Torn, M. S., Park, S.-J., Dolman, H., Mammarella, I., Chae, N., Poyatos, R., López-Blanco, E., Christensen, T. R., Kwon, M. J., Sachs, T., Holl, D., and Luoto, M.: Statistical upscaling of ecosystem CO_2 fluxes across the terrestrial tundra and boreal domain: Regional patterns and uncertainties, Global Change Biology, 27, 4040–4059, http://doi.org/10.1111/gcb.15659, 2021.

Vogel, C., Mueller, C. W., Höschen, C., Buegger, F., Heister, K., Schulz, S., Schloter, M., and Kögel-Knabner, I.: Submicron structures provide preferential spots for carbon and nitrogen sequestration in soils, Nat. Commun., 5, 2947, http://doi.org/10.1038/ncomms3947, 2014.

Vonk, J. E., Mann, P. J., Davydov, S., Davydova, A., Spencer, R. G. M., Schade, J., Sobczak, W. V., Zimov, N., Zimov, S., Bulygina, E., Eglinton, T. I., and Holmes, R. M.: High biolability of ancient permafrost carbon upon thaw, Geophys. Res. Lett., 40, 2689-2693, http://doi.org/10.1002/grl.50348, 2013.

Vonk, J. E., Sanchez-Garcia, L., van Dongen, B. E., Alling, V., Kosmach, D., Charkin, A., Semiletov, I. P., Dudarev, O. V., Shakhova, N., Roos, P., Eglinton, T. I., Andersson, A., and Gustafsson, O.: Activation of old carbon by erosion of coastal and subsea permafrost in Arctic Siberia, Nature, 489, 137-140, http://dx.doi.org/10.1038/nature11392, 2012.

Waldrop, M. P., Wickland, K. P., White III, R., Berhe, A. A., Harden, J. W., and Romanovsky, V. E.: Molecular investigations into a globally important carbon pool: permafrost-protected carbon in Alaskan soils, Global Change Biology, 16, 2543-2554, 10.1111/j.1365-2486.2009.02141.x, 2010.

Wang, X., Wang, C., Cotrufo, M. F., Sun, L., Jiang, P., Liu, Z., and Bai, E.: Elevated temperature increases the accumulation of microbial necromass nitrogen in soil via increasing microbial turnover, Global Change Biology, 26, 5277-5289, https://doi.org/10.1111/gcb.15206, 2020.

Wickland, K. P., Jorgenson, M. T., Koch, J. C., Kanevskiy, M., and Striegl, R. G.: Carbon dioxide and methane flux in a dynamic Arctic tundra landscape: Decadal-scale impacts of ice wedge degradation and stabilization, Geophys. Res. Lett., 47, e2020GL089894, https://doi.org/10.1029/2020GL089894, 2020.

Xu, C., Guo, L., Dou, F., and Ping, C.-L.: Potential DOC production from size-fractionated Arctic tundra soils, Cold Reg. Sci. Technol., 55, 141-150, https://doi.org/10.1016/j.coldregions.2008.08.001, 2009.

Yeloff, D., Bennett, K. D., Blaauw, M., Mauquoy, D., Sillasoo, Ü., van der Plicht, J., and van Geel, B.: High precision 14C dating of Holocene peat deposits: A comparison of Bayesian calibration and wiggle-matching approaches, Quaternary Geochronology, 1, 222-235, https://doi.org/10.1016/j.quageo.2006.08.003, 2006.

Zhang, T., Heginbottom, J. A., Barry, R. G., and Brown, J.: Further statistics on the distribution of permafrost and ground ice in the Northern Hemisphere, Polar Geogr., 24, 126-131, 10.1080/10889370009377692, 2000.